

Acidic Ruthenium PNNP Complexes of Non-enolized 1,3-Dicarbonyl Compounds as Catalysts for Asymmetric Michael Addition

Francesco Santoro, Martin Althaus, Cristina Bonaccorsi, Sebastian Gischig, and Antonio Mezzetti*

Department of Chemistry and Applied Biosciences, ETH Zürich, CH-8093 Zürich, Switzerland

Received March 3, 2008

The chiral dicationic complexes $[\text{Ru}(\mathbf{4a})(\text{PNNP})]^{2+}$ (**2a**) and $[\text{Ru}(\mathbf{4h})(\text{PNNP})]^{2+}$ (**2h**, PNNP is (1*S*,2*S*)-*N,N'*-bis[*o*-(diphenylphosphino)benzylidene]cyclohexane-1,2-diamine), containing non-enolized 2-*tert*-butoxycarbonylcyclopentanone (**4a**) or α -acetyl-*N*-benzyl- δ -valerolactam (**4h**), were prepared from $[\text{RuCl}_2(\text{PNNP})]$ (**1**) by double chloride abstraction with $(\text{Et}_3\text{O})\text{PF}_6$, followed by reaction with the 1,3-dicarbonyl compound. The estimated aqueous pK_a values for **2a** (3.3 ± 0.3) and **2h** (4.7 ± 0.1) were determined by deprotonation with Ph_2NH and pyridine, respectively. The corresponding monocationic enolato complexes **3a** and **3h** were isolated and structurally characterized. Complex **2a** catalyzes the 1,4-addition of **4a** to methyl vinyl ketone with up to 93% ee when a $\text{CH}_2\text{Cl}_2/\text{Et}_2\text{O}$ (1:1) solvent mixture is used. Oxygen-containing cosolvents enhance both the rate and enantioselectivity of the Michael addition with a number of substrates. This observation is discussed in the context of our previous observation that the combined addition of diethyl ether and of β -keto ester **4a** favors and accelerates the deprotonation of **2a** in dichloromethane.

Introduction

The acidity of 1,3-dicarbonyl compounds is widely exploited to form carbon–carbon and carbon–heteroatom bonds, in particular in catalytic processes, such as in conjugate addition reactions.¹ Contrary to other late transition metals such as copper(II) and palladium(II), ruthenium has played a minor role in catalytic asymmetric conjugate addition² until the recent development of chiral amido complexes that catalyze the Michael reaction.^{3,4} These basic complexes are thought to promote the formation of the enolate of the 1,3-dicarbonyl compound, an approach that has been used with other Pd-, Rh-, and Ru-based catalysts.⁵ In an alternative approach, the deprotonation of the 1,3-dicarbonyl compound (usually a β -keto ester) can be achieved by enhancing its acidity via coordination to a Lewis acidic complex, as in the case of the dicationic palladium(II) complexes $[\text{Pd}(\text{OH}_2)_2(\text{P}-\text{P})](\text{OTf})_2$ (P–P = diphosphine).⁶

Our studies of the catalytic properties of ruthenium(II) complexes formed by chloride abstraction from $[\text{RuCl}_2(\text{PNNP})]$ (**1**) (PNNP is (1*S*,2*S*)-*N,N'*-bis[*o*-(diphenylphosphino)benzylidene]cyclohexane-1,2-diamine) have shown that the Ru/PNNP fragment exhibits a highly oxophilic nature.^{7,8} The reaction of $[\text{RuCl}_2(\text{PNNP})]$ with Ag(I)-based halide scavengers (2 equiv) produces poorly defined species that react with water to give dicationic diaqua complexes of the type $[\text{Ru}(\text{OH}_2)_2(\text{PNNP})]^{2+}$.⁹ Furthermore, double chloride abstraction from **1** with $(\text{Et}_3\text{O})\text{PF}_6$ gives an elusive complex, presumably $[\text{Ru}(\text{OEt}_2)_2(\text{PNNP})]^{2+}$, which binds 1,3-dicarbonyl compounds in their non-enolized form. We have briefly reported the complexes $[\text{Ru}(\mathbf{4})(\text{PNNP})]^{2+}$ (**4a** = 2-*tert*-butoxycarbonylcyclopentanone, **2a** or **4h** = α -acetyl-*N*-benzyl- δ -valerolactam, **2h**), which are deprotonated by NEt_3 to give the corresponding enolato derivatives of type **3** (Scheme 1).^{10,11} It should be noted that, in contrast to their enolato analogues, transition metal complexes containing non-enolized 1,3-dicarbonyl compounds are rare, in particular with ruthenium.¹²

* Corresponding author. E-mail: mezzetti@inorg.chem.ethz.ch.

(1) (a) Stowell, J. C. *Carbanions in Organic Synthesis*; Wiley: New York, 1979; Chapter 6. (b) Moreno-Mañas, M.; Marquet, J.; Vallribera, A. *Tetrahedron* **1996**, *52*, 3377. (c) Benetti, S.; Romagnoli, R.; De Risi, C.; Spalluto, G.; Zanirato, V. *Chem. Rev.* **1995**, *95*, 1065.

(2) Christoffers, J.; Koripelly, G.; Rosiak, A.; Rössle, M. *Synthesis* **2007**, 1279.

(3) (a) Ikariya, T.; Murata, K.; Noyori, R. *Org. Biomol. Chem.* **2006**, *4*, 393. (b) Watanabe, M.; Ikgawa, A.; Wang, H.; Murata, K.; Ikariya, T. *J. Am. Chem. Soc.* **2004**, *126*, 11148.

(4) (a) Clapham, S. E.; Guo, R. W.; Zimmer-De Iulius, M.; Rasool, N.; Lough, A.; Morris, R. H. *Organometallics* **2006**, *25*, 5477. (b) Guo, R. W.; Morris, R. H.; Song, D. *J. Am. Chem. Soc.* **2005**, *127*, 516. (c) Guo, R. W.; Chen, X. H.; Elpelt, C.; Song, D. T.; Morris, R. H. *Org. Lett.* **2005**, *7*, 1757.

(5) (a) Culkin, D. A.; Hartwig, J. F. *Acc. Chem. Res.* **2003**, *36*, 234. (b) Slough, G. A.; Bergman, R. G.; Heathcock, C. H. *J. Am. Chem. Soc.* **1989**, *111*, 938. (d) Murahashi, S.-I.; Naota, T.; Taki, H.; Mizuno, M.; Takaya, H.; Komiyama, S.; Mizuho, Y.; Oyasato, N.; Hiraoka, M.; Hirano, M.; Fukuoka, A. *J. Am. Chem. Soc.* **1995**, *117*, 12436.

(6) (a) Hamashima, Y.; Hotta, D.; Sodeoka, M. *J. Am. Chem. Soc.* **2002**, *124*, 11240. For fluorination and Mannich-type reactions, see: (b) Hamashima, Y.; Yagi, K.; Takano, H.; Tamàs, L.; Sodeoka, M. *J. Am. Chem. Soc.* **2002**, *124*, 14530. (c) Hamashima, Y.; Sasamoto, N.; Hotta, D.; Somei, H.; Umebayashi, N.; Sodeoka, M. *Angew. Chem., Int. Ed.* **2005**, *44*, 1525. See also (d) Phua, P. H.; White, A. J. P.; de Vries, J. G.; Hii, K. K. *Adv. Synth. Catal.* **2006**, *348*, 587.

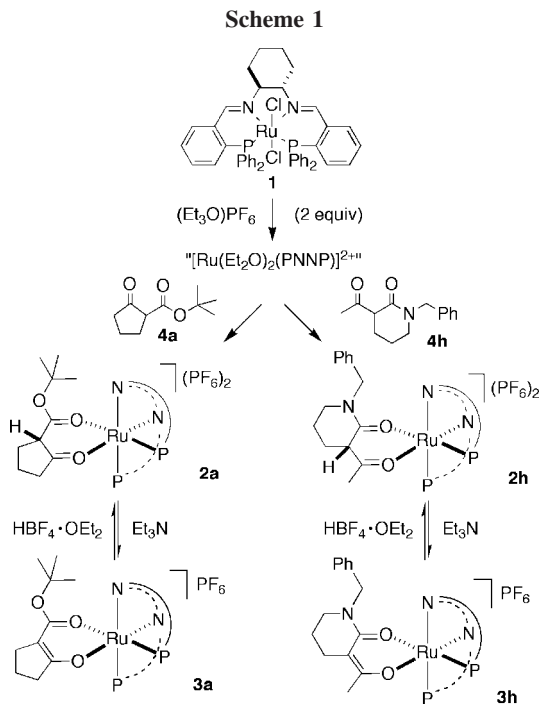
(7) (a) Stoop, R. M.; Bachmann, S.; Valentini, M.; Mezzetti, A. *Organometallics* **2000**, *19*, 4117. (b) Bachmann, S.; Furler, M.; Mezzetti, A. *Organometallics* **2001**, *20*, 2102. (c) Bonaccorsi, C.; Bachmann, S.; Mezzetti, A. *Tetrahedron: Asymmetry* **2003**, *14*, 845. (d) Bonaccorsi, C.; Mezzetti, A. *Organometallics* **2005**, *24*, 4953.

(8) Bonaccorsi, C.; Mezzetti, A. *Curr. Org. Chem.* **2006**, *10*, 225.

(9) Bonaccorsi, C.; Santoro, F.; Gischig, S.; Mezzetti, A. *Organometallics* **2006**, *25*, 2002.

(10) Althaus, M.; Bonaccorsi, C.; Mezzetti, A.; Santoro, F. *Organometallics* **2006**, *25*, 3108.

(11) Bonaccorsi, C.; Althaus, M.; Becker, C.; Togni, A.; Mezzetti, A. *Pure Appl. Chem.* **2006**, *78*, 391.



Beyond their interest to the coordination chemist, **2a** and **2h** are highly relevant to catalytic reactions that exploit the oxophilicity of the Ru/PNNP fragment for the α -heterofunctionalization of 1,3-dicarbonyl compounds, such as the asymmetric hydroxylation¹³ and fluorination¹⁴ of β -keto esters and β -keto amides. As β -keto ester complexes of late transition metals are known to catalyze conjugate addition reactions,^{2–4,6a} we also successfully applied our ruthenium PNNP complexes in the Michael addition of β -keto esters to methyl vinyl ketone. The study of this reaction in a catalytic and stoichiometric fashion revealed interesting mechanistic features related to the acid–base equilibrium between the β -keto ester complex **2a** and its enolato analogue **3a**. The results of our investigations are reported in full below.

Results and Discussion

2-tert-Butoxycarbonylcyclopentanone Derivatives. The reaction of $[\text{RuCl}_2(\text{PNNP})]$ (**1**) with $(\text{Et}_3\text{O})\text{PF}_6$ (2 equiv), followed by addition of 2-tert-butoxycarbonylcyclopentanone (**4a**, 1 equiv) to the resulting CD_2Cl_2 solution, gives the dicationic adduct $(\Lambda)\text{-}(\text{S},\text{S},\text{S})\text{-}[\text{Ru}(\text{4a})(\text{PNNP})]^{2+}$ (**2a**) as a single detectable diastereoisomer (Scheme 1 left). The absolute configuration of **2a** is assigned on the basis of NMR spectroscopic studies that allow correlating the X-ray structure of the enolato analogue

(12) (a) Sahai, R.; Kabisatpathy, A. K.; Petersen, J. D. *Inorg. Chim. Acta* **1986**, *115*, L33. A complex claimed to contain non-enolized *N,N'*-diphenylmalonamide is probably a Ru(III) enolato complex, as it has been reported to be paramagnetic; (b) Blum, J.; Fisher, A.; Greener, E. *Tetrahedron* **1973**, *29*, 1073. For an overview on different coordination modes of 1,3-dicarbonyl ligands and examples of Ni(II), Co(II), Cu(II), and Zn(II) complexes with acetylacetonone, malonate, and malonamide, see: (c) Kawaguchi, S. *Coord. Chem. Rev.* **1986**, *70*, 51. (d) Yamazaki, S. *Heterogeneous Chem. Rev.* **1995**, *2*, 103. (e) Cramer, R. E.; Cramer, S. W.; Cramer, K. F.; Chudyk, M. A.; Seff, K. *Inorg. Chem.* **1977**, *16*, 219. (f) Rodríguez-Martín, Y.; Luis, P. A. L.; Ruiz-Pérez, C. *Inorg. Chim. Acta* **2002**, *328*, 169.

(13) Toullec, P. Y.; Bonaccorsi, C.; Mezzetti, A.; Togni, A. *Proc. Natl. Acad. Sci. U.S.A.* **2004**, *101*, 5810.

(14) Althaus, M.; Becker, C.; Togni, A.; Mezzetti, A. *Organometallics* **2007**, *26*, 5902.

(15) A $\text{p}K_{\text{a}}$ of -3.6 has been proposed for Et_2OH^+ : Arnett, E. M.; Wu, C. Y. *J. Am. Chem. Soc.* **1960**, *82*, 4999.

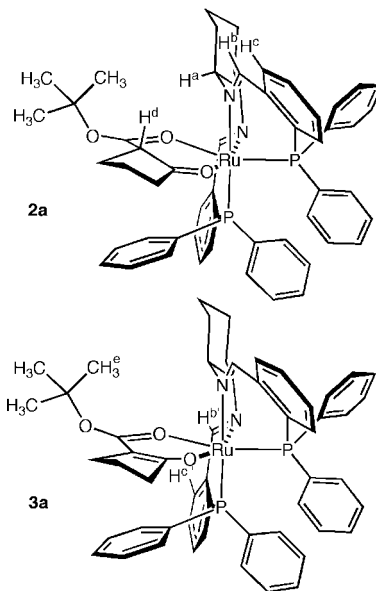


Figure 1. Hydrogen atoms involved in selected NOE contacts in **2a** and **3a**.

3a with the solution structure of both complexes as described below. Complex **2a** was characterized in solution, as it decomposes upon isolation by precipitation or concentration, and all crystallization attempts yielded the dicationic acid complex $[\text{Ru}(\text{5})(\text{PNNP})]^{2+}$ (**6**) (**5** = 2-oxo-1-cyclopentanecarboxylic acid) instead.

In the dicationic complex **2a**, the non-enolized β -keto ester **4a** is bound in its keto form, as indicated by the ^1H NMR signal of the methine proton H^{d} at δ 3.78 (δ 3.04 in free β -keto ester **4a**) (Figure 1, all complex charges are omitted). The one-bond $^{13}\text{C}\text{--}^1\text{H}$ HMQC spectrum unambiguously supports the assignment of this signal to H^{d} , as it binds to the 2-carbon atom ($\text{C}\text{--}\text{H}^{\text{d}}$), whose sp^3 -hybridization is confirmed by its chemical shift ($\delta(^{13}\text{C}) = 55.5$). Furthermore, the long-range $^{13}\text{C}\text{--}^1\text{H}$ HMQC spectrum shows that H^{d} correlates with both carbonyl carbons and with the adjacent methylene group of the cyclopentanone ring.

The deprotonation of **2a** with Et_3N (1 equiv) gives the corresponding monocationic enolato complex **3a** as a single diastereoisomer, which was isolated as an air-stable solid (Scheme 1 left). Both NMR spectroscopy and the X-ray study discussed below indicate that **3a** contains the deprotonated β -keto ester **4a** in its enolate form. Accordingly, the δ 3.78 region of the ^1H NMR spectrum shows no signal that might be assigned to the methine proton. A ^{13}C NMR resonance at δ 93.1 is assigned to the enolic C^2 carbon atom, whereas the $\text{C}\text{--}\text{H}^{\text{d}}$ signal at δ 55.5 observed for **2a** is absent. The addition of $\text{HBF}_4\cdot\text{OEt}_2$ (1 equiv)¹⁵ to a CD_2Cl_2 solution of **3a** reverses the reaction and produces **2a** quantitatively.

As all attempts to obtain X-ray quality crystals of enantiomerically pure $(\text{S},\text{S})\text{-2a}$ failed, we prepared the corresponding racemate $(\text{rac})\text{-2a}$ by protonation of $(\text{rac})\text{-3a}$ ¹⁶ with $\text{HBF}_4\cdot\text{Et}_2\text{O}$ in CD_2Cl_2 . Slow diffusion of toluene into the resulting solution (in an NMR tube kept in a glovebox under purified nitrogen during several weeks) gave orange crystals that an X-ray study revealed to contain $(\text{rac})\text{-}[\text{Ru}(\text{5})(\text{PNNP})]^{2+}$ (**6**), a complex featuring the non-enolized 2-oxo-1-cyclopentanecarboxylic acid (**5**) as ligand (Figure 2, charges are not shown). The carboxylic

(16) Containing the racemic PNNP ligand prepared from $(\text{rac})\text{-trans-1,2-diaminocyclohexane}$.

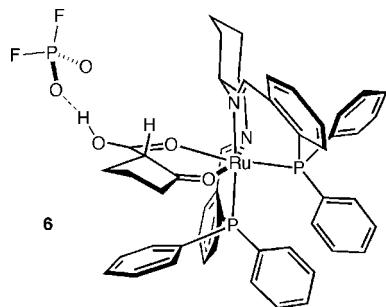


Figure 2. Outline of the solid-state structure of **6** (the hydrogen bond between the carboxylic group and the $[\text{PF}_2\text{O}_2]^-$ anion is highlighted).

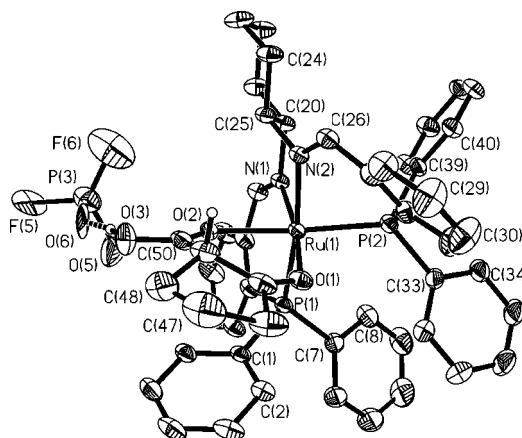


Figure 3. ORTEP drawing of **6**.

acid is probably formed by isobutene elimination from β -keto ester **4a**, a reaction that can be catalyzed by traces of acid. Although it is not the desired product, **6** will be discussed here because it is a rare example of a ruthenium complex containing a non-ionized carboxylic acid¹⁷ and, more importantly, a useful model for **2a**. To the best of our knowledge, there are no structural data of ruthenium complexes that contain non-enolized β -keto esters, the closest analogues being complexes featuring a weakly C-bound acetylacetonato ligand.¹⁸

X-ray Structure of (rac)-6. The asymmetric unit of the centrosymmetric crystal ($P2_1/n$ space group) contains one enantiomer of the dicationic complex (the other one being generated by the crystallographic inversion center), one $[\text{BF}_4]^-$ anion, and three sites that are partially occupied by highly disordered $[\text{BF}_4]^-$ and $[\text{PF}_2\text{O}_2]^-$ anions, the latter from hexafluorophosphate hydrolysis. The coordination of ruthenium is distorted octahedral with the PNNP ligand in *cis- β* configuration, which is Λ for the *S,S*-enantiomer of the ligand (Figures 2 and 3). The enolizable hydrogen atom on C(49) is located on the unshielded *re* face of the configurationally labile, *O,O*-bidentate 2-oxo-1-cyclopentanecarboxylic acid, which has, therefore, the *S*-configuration. The carbon–oxygen distances indicate that the COOH group is coordinated with the carbonyl oxygen atom to ruthenium (Table 1). The acidic hydrogen on O(3) is involved in a strong hydrogen bond to one of the $[\text{PF}_2\text{O}_2]^-$ anions. Both

Table 1. Selected Bond Lengths (Å) and Angles (deg) for **3a** and **6**

	3a	6
Ru(1)–P(1)	2.2803(8)	2.2994(10)
Ru(1)–P(2)	2.2681(8)	2.2651(10)
Ru(1)–N(1)	2.044(2)	2.046(3)
Ru(1)–N(2)	2.097(2)	2.091(3)
Ru(1)–O(1)	2.082(2)	2.106(3)
Ru(1)–O(2)	2.144(2)	2.168(3)
C(45)–O(1)	1.281(4)	1.230(6)
C(45)–C(49)	1.383(4)	1.512(8)
C(49)–C(50)	1.411(4)	1.469(11)
C(50)–O(2)	1.259(4)	1.224(6)
C(50)–O(3)	1.332(4)	1.348(7)
O(3)···O(6)		2.641(17)
O(3)···O(6')		2.651(17)
P(1)–Ru(1)–P(2)	104.58(3)	104.02(4)
P(1)–Ru(1)–N(1)	94.5(7)	93.68(9)
P(1)–Ru(1)–N(2)	172.17(7)	171.81(10)
P(1)–Ru(1)–O(1)	92.40(6)	90.48(8)
P(1)–Ru(1)–O(2)	85.40(6)	85.34(8)
P(2)–Ru(1)–N(1)	102.30(7)	102.39(9)
P(2)–Ru(1)–N(2)	82.59(7)	83.19(9)
P(2)–Ru(1)–O(1)	85.76(6)	86.63(9)
P(2)–Ru(1)–O(2)	169.52(6)	168.46(9)
N(1)–Ru(1)–N(2)	80.60(10)	80.74(12)
N(1)–Ru(1)–O(1)	167.61(9)	168.81(12)
N(1)–Ru(1)–O(2)	79.70(9)	83.44(13)
N(2)–Ru(1)–O(1)	91.28(9)	93.96(12)
N(2)–Ru(1)–O(2)	87.64(9)	88.06(12)
O(1)–Ru(1)–O(2)	90.70(8)	86.55(12)

Figures 2 and 3 depict (Λ)-(*S,S,S*)-**6**, which contains the same (*S,S*) PNNP enantiomer used in catalysis, and the difluorophosphate anion involved in the hydrogen bond (only the major conformation of the disordered anion is shown).

To the best of our knowledge, this is the first structurally characterized complex of an enolizable β -keto acid featuring *O,O*-bidentate coordination and a dangling OH group, whereas some μ -carboxylato diruthenium complexes containing carbonyl-*O*-bound benzoic acid have been reported.^{17a–c} It should be noted that phosphine complexes of ruthenium exhibit a low oxophilicity and do not bind oxygen donors, unless hard co-ligands are present.¹⁹ Therefore, **6** is a further indication that the nitrogen donors of the PNNP ligand enhance the oxophilicity of ruthenium.⁸

X-ray Structure of 3a. After unsuccessful attempts to get X-ray quality crystals of enantiomerically pure **3a**, the corresponding racemic derivative readily crystallized by diffusion of pentane into a CH_2Cl_2 solution of (*rac*)-**3a**.¹⁶ The crystal analyzed belongs to the centrosymmetric space group $P\bar{1}$. The asymmetric unit contains two crystallographically independent complex molecules and $[\text{PF}_6]^-$ anions, as well as severely disordered dichloromethane molecules distributed over four different sites. As the two complex cations around Ru(1) and Ru(2) possess very similar metrical parameters, only one is discussed in full (Figure 4, Table 1).

The coordination of ruthenium is distorted octahedral with the PNNP ligand in *cis- β* configuration, which is Λ in the enantiomer containing (*S,S*)-PNNP (Figure 4). The enolato ligand is close to perfect planarity. The ester carbon atom C(50) exhibits the largest deviations from the least-squares enolate plane, and the Ru(1) atom is displaced from the plane of the enolate and away from the C(1)–C(6) phenyl group on P(1) by 0.188(4) Å. The C(1)–C(6) phenyl shields the *si* face of the

(17) (a) Rotem, M.; Shvo, Y.; Goldberg, I.; Shmueli, U. *Organometallics* **1984**, *3*, 11–1758. (b) Rotem, M.; Goldberg, I.; Shmueli, U.; Shvo, Y. *J. Organomet. Chem.* **1986**, *314*, 1–185. (c) Spohn, M.; Strahle, J.; Hiller, W. *Z. Naturforsch. B.* **1986**, *41*, 541 See also. (d) Steines, S.; Englert, U.; Driessen-Hölscher, B. *Chem. Commun.* **2000**, 217.

(18) See, for instance: (a) Koelle, U.; Rietmann, C.; Raabe, G. *Organometallics* **1997**, *16*, 3273. (b) Shono, J.; Nimura, Y.; Hashimoto, T.; Shimizu, K. *Chem. Lett.* **2004**, *33*, 1422.

(19) (a) Mezzetti, A.; Becker, C. *Helv. Chim. Acta* **2002**, *85*, 2686. (b) Becker, C.; Kieltch, I.; Brogini, D.; Mezzetti, A. *Inorg. Chem.* **2003**, *42*, 8417.

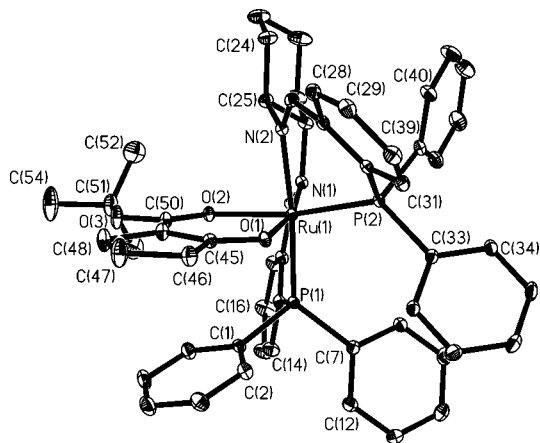


Figure 4. ORTEP drawing of **3a**.

enolato ligand, leaving the *re* face accessible to electrophilic attack, whose stereochemical implications in catalysis will be discussed later.

The coordination bond lengths reflect the *trans* influence of the ligands, which decreases along the series P > N > O. Thus, the P(2) atom (*trans* to O) is significantly closer to ruthenium than P(1) (*trans* to N) (2.2681(8) vs 2.2803(8) Å) because of the lower *trans* influence of oxygen with respect to nitrogen. The effect on the Ru–N bond lengths is even larger (Table 1). In the enolato ligand, the C(45)–O(1) and C(50)–O(2) distances (1.281(4) and 1.259(4) Å, respectively) indicate that the keto-derived CO has a stronger single-bond character than the CO of the ester group. Therefore, O(1) carries a larger negative charge and binds stronger to Ru(1) than O(2), which explains why it is *trans* to nitrogen rather than to phosphorus.

Apart from the dicarbonyl(ato) ligand, the structures of **6** and **3a** (Figures 3 and 4) show close analogies (Table 1), which will be useful in the discussion of the stereochemistry of the Michael reaction. The most important common feature is that the 1,3-dicarbonyl compound binds to ruthenium with the ketone carbonyl group *trans* to N(1) in both complexes. In the case of **3a**, both steric and electronic factors favor this orientation, as (a) the bulky *tert*-butyl points away from the PPh₂ group on P(1) and (b) the stronger donating oxygen atom, O(1), is *trans* to the donor with the weaker *trans* influence between N and P, that is, the nitrogen donor N(1). The same arrangement is kept in complex **6**, despite the fact that the bulky *tert*-butyl group is missing and that the electronic asymmetry is much less pronounced in the (non-enolized) β -keto acid of **6** than in the enolate of complex **3a**. This is an important point, as it shows that no major structural change occurs upon deprotonation of the β -keto ester, which allows correlating the solution structure of **2a** with the X-ray structure of **3a**.

Solution Structure of 2a. Both **2a** and **3a** show NOE contacts of the H^c atoms in the *tert*-butyl group of the β -keto ester to one imine hydrogen (H^{b'}) and to H^{c'} of the PNNP backbone (Figure 1, the atoms involved in the above contacts are shown only in **3a** for simplicity). This suggests that **2a** and **3a** have similar structures and the same relative configuration. Additionally, the NOESY experiment of **2a** shows contacts between the methine hydrogen of the β -keto ester (H^d) and three protons of the PNNP ligand, namely, H^a, the H atom α to one nitrogen, the imine hydrogen H^b, and one *ortho*-hydrogen (H^c), indicating that H^d points up toward the cyclohexane backbone of the PNNP ligand (Figure 1, **2a**).

α -Acetyl Lactam Complexes. Treatment of the dichloro complex **1** with (Et₃O)PF₆ (2 equiv) in CD₂Cl₂, followed by

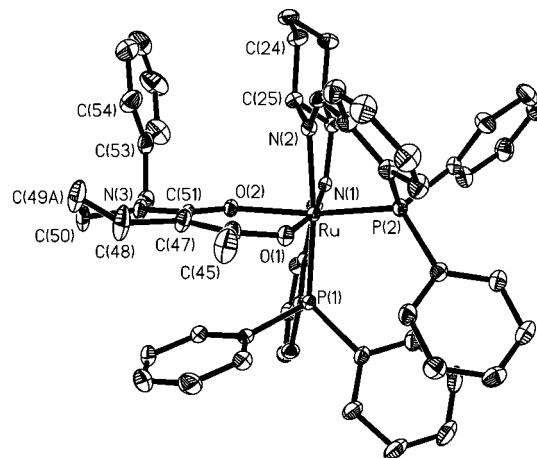


Figure 5. ORTEP drawing of **3h**.

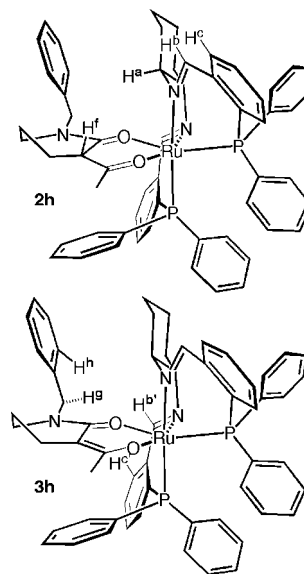


Figure 6. Hydrogen atoms involved in selected NOE contacts in **2h** and **3h**.

addition of α -acetyl-*N*-benzyl- δ -valerolactam (**4h**, 1 equiv), gives the dicationic adduct [Ru(**4h**)(PNNP)]²⁺ (**2h**), which contains non-enolized **4h** in its keto form. A single diastereoisomer was detected in solution by ¹H and ³¹P NMR spectroscopy. Unlike **2a**, **2h** can be isolated in the solid state and was, therefore, fully characterized. Although all attempts to get X-ray quality crystals failed, the formulation of **2h** is unambiguously supported by analytical and NMR spectroscopic data and by comparison with the enolato analogue **3h**, which was characterized crystallographically (Figure 5). Diagnostic signals of **2h** are the ¹H NMR doublet of doublets of the enolizable proton H^f at δ 3.63 and the ¹³C NMR resonance of the corresponding sp³ carbon atom at δ 50.5, which were assigned as described for **2a** (Figure 6, charges of complexes not shown).

Preliminary tests showed that complex **2h** is less acidic than **2a** and identified pyridine as adequate reference. The pK_a determination²⁰ gave an average estimated value of 4.67 \pm 0.08

(20) (a) All pK_a data were measured in CD₂Cl₂ against a reference of known aqueous pK_a (see Experimental Section) with the method introduced by Morris for the estimation of aqueous pK_a values of hydride and dihydrogen complexes in nonaqueous solvents.^{20b} (b) Jia, G.; Morris, R. H. *Inorg. Chem.* **1990**, *29*, 581. See also: (c) Kristjansdottir, S. S.; Norton, J. R.; In *Transition Metal Hydrides*; Dedieu, A., Ed.; VCH: Weinheim, 1992; p 324.

Table 2. Selected Bond Lengths (Å) and Angles (deg) for **3h**

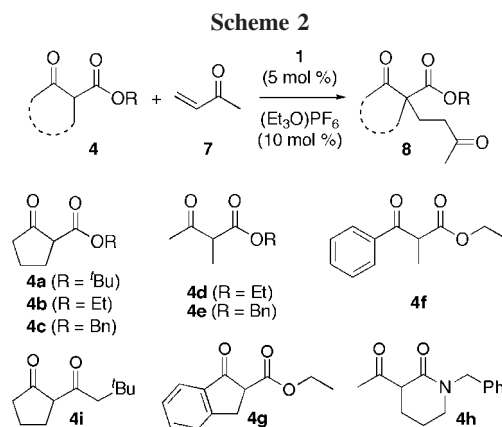
Ru(1)–P(1)	2.2855(12)	Ru(1)–P(2)	2.2785(12)
Ru(1)–N(1)	2.055(4)	Ru(1)–N(2)	2.098(4)
Ru(1)–O(1)	2.045(3)	Ru(1)–O(2)	2.103(3)
C(46)–O(1)	1.291(5)	C(46)–C(47)	1.389(7)
C(47)–C(51)	1.443(7)	C(51)–O(2)	1.269(5)
P(1)–Ru(1)–P(2)	104.33(4)	P(1)–Ru(1)–N(1)	93.85(10)
P(1)–Ru(1)–N(2)	171.39(11)	P(1)–Ru(1)–O(1)	91.90(10)
P(1)–Ru(1)–O(2)	85.96(9)	P(2)–Ru(1)–N(1)	105.57(10)
P(2)–Ru(1)–N(2)	83.73(11)	P(2)–Ru(1)–O(1)	83.13(9)
P(2)–Ru(1)–O(2)	166.40(9)	N(1)–Ru(1)–N(2)	80.88(14)
N(1)–Ru(1)–O(1)	168.00(13)	N(1)–Ru(1)–O(2)	82.18(13)
N(2)–Ru(1)–O(1)	92.09(14)	N(2)–Ru(1)–O(2)	86.57(13)
O(1)–Ru(1)–O(2)	87.73(12)		

(on the aqueous scale). For comparison, we estimate a pK_a^{aq} of about ~ 14 – 15 for the α -acyl lactam **4h** on the basis of the pK_a value of *N,N*-dimethyl acetylamine measured in DMSO (18.2)²¹ for 3-oxobutanoic acid ethyl ester and considering the pK_a difference between the DMSO and H₂O acidity scales.

A striking feature of the formation of **2h** is that α -acyl lactam **4h**, which is present in its tautomeric enol form to 66% in CDCl₃,¹³ is quantitatively converted to the keto form upon coordination to ruthenium rather than forming an enolato complex. To understand this, one has to keep in mind that α -acyl lactam **4h** is considerably less acidic than β -keto ester **4a** (~ 14 – 15 vs 10.5, see below). Therefore, the corresponding enolato complex **3h** can be reasonably expected to be more basic than **3a**, which favors its protonation to **2h**. As α -acyl lactam **4h** can bind to ruthenium only in its keto form (and not as enol), the coordination to the metal has the seemingly paradoxical overall effect of forcing the keto–enol tautomer equilibrium of **4h** toward the keto form. However, the coordination to the dicationic Ru/PNNP fragment dramatically enhances the acidity of **4h** (by 9–10 orders of magnitude).

Finally, the enolato analogue **3h** was prepared by deprotonation of **2h** with NEt₃ (Scheme 1 right) and fully characterized (see Experimental Section), including an X-ray study. Orange crystals of (*rac*)-**3h**¹⁶ were grown from pentane/CH₂Cl₂. The centrosymmetric (*P*₁) crystal of (*rac*)-**3h** features an asymmetric unit containing the complex cation, one [PF₆][−] anion, and three disordered CH₂Cl₂ molecules (Figure 5, Table 2). The enolate is planar within $\pm 0.044(3)$ Å and is slightly tilted away from the phenyl ring on P(1) that shields the *si* face of the enolate. Therefore, the ruthenium atom is located above the least-squares plane of the enolate (by 0.209(5) Å). The C–C and C–O distances suggest that the ketone carbonyl oxygen O(1) bears the higher negative charge. The six-membered ring of lactam **4h** has an envelope conformation, with the out-of-plane atom C(49) disordered over two positions at 87:13 occupancy. Only the major conformer is shown in Figure 5.

A further important structural feature is the conformation of the benzyl substituent on N(3), which points toward the cyclohexane ring. The NOESY NMR experiments show that **3h** retains this conformation in solution and that **2h** also exists in the same conformation in CD₂Cl₂. In both complexes, the endo benzylic hydrogen (H^a) and the *N*-benzyl *ortho*-H (H^b) of α -acyl lactam **4h** display NOE contacts to the imine hydrogen H^{b'} and to H^{c'} of the PNNP backbone (shown only for **3h** in Figure 6 for simplicity). Therefore, **2h** and **3h** have similar structures in solution. Additionally to the aforementioned contacts, the enolizable hydrogen H^f of **2h** displays NOE



contacts to H^a, H^b, and H^c (Figure 6 top). Therefore, it must point up toward the cyclohexane backbone.

In general, complexes featuring non-enolized 1,3-dicarbonyl compounds as ligands are rare, in particular with **4d** and **5d** metals.^{12c–f} To the best of our knowledge, besides **2a** and **2h**, the only other complex that can be safely regarded as a ruthenium(II) complex containing a non-enolized 1,3-dicarbonyl compound is $[\text{Ru}(\text{NH}_3)_4(\text{acacH})]^{2+}$.^{12a} In the same group, iron(III) complexes containing non-enolized β -keto esters have been observed in the gas phase by ESI-MS.²² However, it has been reported that β -keto esters react with aqueous Fe(III) solutions to give enolato complexes even in the presence of Brønsted acids.²³

Catalytic Michael Addition. The 1,3-dicarbonyl complexes formed *in situ* upon double chloro abstraction from complex **1** catalyze the Michael addition of **4a–i** to methyl vinyl ketone (**7**) (Scheme 2). For a preliminary screening, dichloro complex **1** was treated with $(\text{Et}_3\text{O})\text{PF}_6$ (2 equiv) in CH₂Cl₂ at room temperature during 16 h. Then, the 1,3-dicarbonyl compound and the enone **7** (20 equiv vs Ru each) were added, and the resulting solution was stirred during 24 h. After this time, the reaction solution was analyzed by quantitative gas chromatography, and the products **8a–i** were isolated and characterized (see Experimental Part).

As already observed in the asymmetric fluorination of β -keto esters with the Ru/PNNP catalyst,¹⁴ the best results in terms of product yield and enantioselectivity were obtained with 2-*tert*-butoxycarbonylcyclopentanone (**4a**), which gave the Michael adduct **8a** with 79% ee without optimization (Table 3, run 1). Therefore, all the mechanistic studies described below were performed with this substrate. Under the same conditions, the acyclic substrates **4d–f** gave much lower enantioselectivity and moderate yields after the same reaction time (runs 5–7), independently of the substitution pattern of the 1,3-dicarbonyl compound.

An interesting observation is that the reactions with **4d–f** do not go to completion even after 72 h but stop after 48 h at 50–60% yield. Surprisingly, α -acyl lactam **4h** and β -keto ester **4g** (runs 8, 9), which have a high enol content (66% for **4h**, 33% for **4g**), gave the corresponding Michael adducts with high conversion and yield but no enantioselectivity. This result might suggest a non-metal-catalyzed, background reaction. However, a control reaction showed that these substrates do not react spontaneously with methyl vinyl ketone at room temperature in CD₂Cl₂ even after 2 days, as indicated by NMR spectroscopy.

(22) Trage, C.; Schröder, D.; Schwarz, H. *Chem.–Eur. J.* **2005**, *11*, 619.

(23) Pelzer, S.; Kauf, T.; van Wüllen, C.; Christoffers, J. *J. Organomet. Chem.* **2003**, *684*, 308.

Table 3. Catalytic Michael Addition of Different Donors to Methyl Vinyl Ketone^a

run	Michael donor	yield (%)	ee (%)
1	4a	94	79 (<i>R</i>)
2 ^b	4a	88	85 (<i>R</i>)
3	4b	95	40
4	4c	quant.	44
5	4d	59	10 ^c
6	4e	49	29
7 ^d	4f	26	60
8	4g	quant.	<i>rac</i>
9	4h	81	<i>rac</i>
10	4i	93	20

^a Reaction conditions: The catalyst precursor **1** (30 mg, 36 μmol, 5 mol %) was treated with Et₃OPF₆ (2 equiv) in CH₂Cl₂, 24 h reaction time unless otherwise stated. ^b The catalyst (5 mol %) was generated by protonation of **3a** with HBF₄·Et₂O (1 equiv) in CH₂Cl₂. ^c By optical rotation. ^d Reaction time 72 h.

Table 4. Screening of Chloride Scavengers (MY) in the Michael Addition of **4a^a**

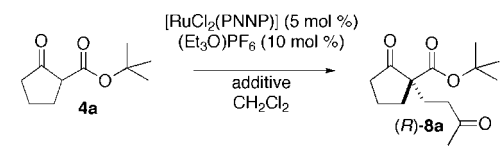
run	MY	MY:Ru ratio	time (h)	conv (%)	yield (%)	ee (%)
1	(Et ₃ O)PF ₆	2	24	97	94	79
2	AgPF ₆	2	24	96	96	75
3	(Et ₃ O)BF ₄	2	24	93	71	40
4	(Me ₃ O)BF ₄	2	24	93	81	58
5	AgBF ₄	2	24	89	70	71
6	AgSbF ₆	2	24	81	46	24

^a In runs 1, 3, and 4, **1** was activated by reaction with the given oxonium salt in CH₂Cl₂ for 18 h. The catalyst solution was then used directly. In runs 2, 5, and 6, **1** was stirred with the given silver salt in CH₂Cl₂ for 18 h, and the catalyst solution was filtered over dried Celite in a glovebox before use.

Finally, diketone **4i** gave the corresponding Michael product in high yield but with low enantioselectivity (20% ee, run 10). As **4i** and **4a** are sterically similar, the difference probably originates from electronic factors and may involve the higher acidity of diketone **4i** compared to β-keto ester **4a**. This result is in sharp contrast to the reaction catalyzed by Sodeoka's palladium catalyst, which converted the same diketone **4i** to the Michael product in 89% yield and 90% ee.^{6a}

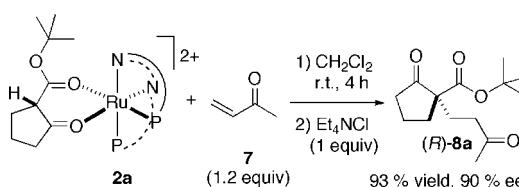
In an effort to improve the enantioselectivity, we found that the catalyst generated by protonation of the isolated enolato complex **3a** with HBF₄·Et₂O (1 equiv) produced the Michael adduct **8a** with 85% ee (run 2). As this result might suggest an anion effect on the enantioselectivity, as previously observed in the cyclopropanation of olefins with Ru/PNNP complexes,^{7d} we screened different oxonium and silver(I) salts as chloride scavengers in the Michael addition of **4a** to **7** (Table 4). It should be noted that the silver(I) salts AgY (Y = SbF₆, PF₆, or BF₄) (2 equiv) are known to abstract both chloro ligands from **1** even in the absence of oxygen donors.⁹ Furthermore, we have previously ascertained that addition of β-keto ester **4a** to these solutions produces **2a**, as indicated by the ³¹P NMR spectra of the reaction solutions.¹⁴

The best performing system remains (Et₃O)PF₆ (run 1), all other scavengers giving lower yield and enantioselectivity. In particular, AgSbF₆ gave surprisingly low activity and selectivity (run 6). Overall, the data in Table 4 are indicative of anion effects, but the results concerning the tetrafluoroborate complexes (runs 3–5) show that also oxygen donors affect the enantioselectivity. In fact, when an oxonium salt (R₃O)Y is used for chloride abstraction, an equivalent amount of the corresponding ether OR₃ is formed, which might affect the reaction either by coordinating to ruthenium or by acting as a base (see below). Therefore, we studied the effect of oxygen-containing additives in more detail (Table 5).

Table 5. Study of the Effect of Oxygen-Containing Additives^a


run	additive/solvent	time (h)	yield (%)	ee (%)
1	H ₂ O ^b	24	93	75
2	Et ₂ O/CH ₂ Cl ₂ (1:1)	18	>99	93
3	TBME/CH ₂ Cl ₂ (1:1)	18	>99	91
4	dioxane/CH ₂ Cl ₂ (1:1)	24	53	83

^a See Table 3 for reaction conditions. TBME = *tert*-butyl methyl ether. ^b Complex **1** was activated with AgBF₄ (2 equiv) under ether-free conditions, then H₂O (2 equiv vs catalyst) was added.

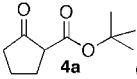
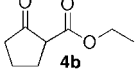
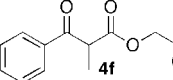
Scheme 3

Effect of Oxygen-Containing Co-solvents. We first tested the previously reported⁹ diaqua complex [Ru(OH)₂(PNNP)]²⁺ as catalyst, which was prepared by activation of **1** with AgBF₄ (2 equiv) in CH₂Cl₂, followed by addition of water (2 equiv). Upon adding β-keto ester **4a** (20 equiv) to this solution, the catalyst solution turned red again, which suggests that the keto ester adduct **2a** is formed. The reaction with methyl vinyl ketone (20 equiv) gave the Michael adduct with 75% ee after 24 h (Table 5, run 1), which is similar to the result obtained with the 1/2 (Et₃O)PF₆ catalyst (Table 3, run 1).

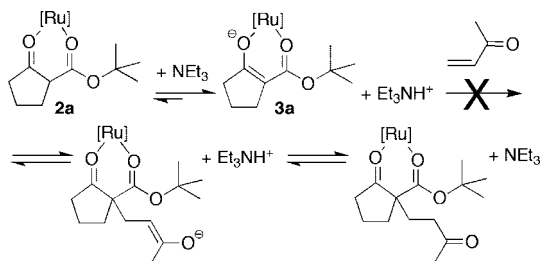
In the case of oxygen-containing co-solvents, 1:1 mixtures of CH₂Cl₂ and of the co-solvent were used, as the catalyst is insoluble in ethers (and alcohols). The concentrations of catalyst (18 mM) and substrates (360 mM) were kept constant throughout the screening. With diethyl ether or *tert*-butyl methyl ether (TBME), the Michael product was formed quantitatively after 18 h and with excellent enantioselectivity (up to 93% ee in the case of Et₂O) (Table 5, runs 2 and 3). Contrary to water, all ethers tested improve the enantioselectivity as compared to CH₂Cl₂, the lower value being obtained with 1,4-dioxane (83% ee), which also gives a lower yield (53% after 24 h, run 4). As ethers are known to bind to the Ru/PNNP fragment,^{7,8} we speculate that dioxane binds strongly to ruthenium, thereby reducing its catalytic performance. Overall, these findings suggest that weakly coordinating, oxygen-containing co-solvents (such as ethers) influence the rate and the enantioselectivity of the catalytic reaction. Thus, the Michael addition of selected β-keto esters was studied in CH₂Cl₂/Et₂O (1:1), the best performing solvent mixture. With all the tested substrates, both the activity and the enantioselectivity are improved, albeit to a different extent (Chart 1). Investigations aimed at understanding this effect are described below.

Mechanistic Considerations. As complexes **2a** and **3a** are obvious candidates as intermediates of the catalytic cycle, we studied their stoichiometric reactions with methyl vinyl ketone (**7**). When **7** (1.2 equiv) is added to a CH₂Cl₂ solution of **2a** (formed *in situ* as described above) in an NMR tube, the Michael adduct **8a** is formed in 93% yield and with 90% ee after 4 h of reaction time (Scheme 3), as indicated by GC and chiral HPLC analysis after workup with NEt₄Cl (2 equiv) to displace the Michael adduct **8a** from the catalyst. The ¹H NMR spectra of

Chart 1

	solvent	reaction time (h)	yield (%)	ee (%)
	CH ₂ Cl ₂	24	94	79
	CH ₂ Cl ₂ /Et ₂ O (1:1)	18	>99	93
	CH ₂ Cl ₂	24	95	40
	CH ₂ Cl ₂ /Et ₂ O (1:1)	18	>99	63
	CH ₂ Cl ₂	72	26	60
	CH ₂ Cl ₂ /Et ₂ O (1:1)	72	41	85

Scheme 4

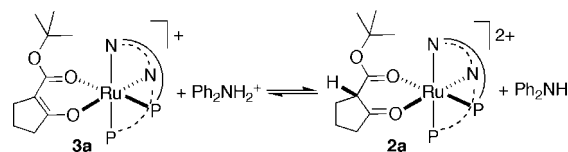


the reaction solution show the disappearance of **2a** and the formation of **8a**, whereas the ³¹P NMR spectrum remains invariant during the reaction time. Our interpretation of the latter observation is that **8a** remains coordinated to ruthenium after its formation to give [Ru(**8a**)(PNNP)]²⁺, whose ³¹P NMR spectrum is indistinguishable from that of **2a**. As for the stereochemical issues of the reaction, it should be noted that the *R* absolute configuration of **8a** is consistent with the *re* face attack of the β -keto ester, which is the accessible enantioface both in **2a** and in **3a** (Figure 1). The enantiomeric excess observed in the stoichiometric reaction is close to that of the best catalytic reaction (93% ee, Table 5, run 2).

In contrast, the enolato complex **3a** does not react with methyl vinyl ketone (**7**) (1 equiv, 48 h, CD₂Cl₂). Furthermore, no reaction occurs when **2a** is treated with a stoichiometric amount of **7** in the presence of NEt₃ as base (B), which gives, besides BH⁺ (1 equiv), **3a** as the only detectable complex. This observation rules out a mechanism in which the enolato complex **3a** reacts with **7** to give an intermediate enolate, which would be basic enough²⁴ to deprotonate Et₃NH⁺ (p*K*_a = 10.8)²⁵ present in the reaction solution and to give the Michael product **8** after tautomerization (Scheme 4). We conclude that the enone **7** is too weak an electrophile to react without activation by a strong acid. The effect of base on the catalytic reactions reinforces the above line of reasoning. In fact, NEt₃ (1 equiv vs **2a**) shuts down the catalytic reaction, **8a** being formed in less than 6% yield after 72 h.

Similarly to our finding with **3a**, Sodeoka reported that the palladium(II) enolato complex [Pd(**4i'**)(P–P)]⁺ (**4i'** is the enolate of **4i**) does not react with **7**. It should be noted that a weak acid is present in this case too, namely, water (1 equiv), which is formed by reaction of **4i** with the binuclear palladium hydroxo complex [Pd₂(μ -OH)₂(P–P)₂]²⁺ (P–P = chiral diphosphine).^{6a} As the Michael addition smoothly occurs to give **8** upon addition of triflic acid to the palladium enolato complex, it was suggested that the role of the acid is to activate the enone toward

Scheme 5



nucleophilic attack by the enolato complex.^{6a} However, it seemed unlikely to us that such an explanation would hold for the ruthenium system, as, on the basis of the p*K*_a value between 2 and 5 estimated for **2a**,¹⁰ we anticipated that the α -hydrogen of the ruthenium-bound β -keto ester would not be acidic enough to protonate methyl vinyl ketone²⁶ to such an extent to trigger the 1,4-addition. An alternative mechanism based on the activation of the enone toward nucleophilic attack by coordination to the metal, as suggested for the iron(III)-catalyzed Michael addition,²³ seemed also improbable, as **3a** is a coordinatively saturated complex.

At this point, it should be noticed that many catalysts for the Michael addition of 1,3-dicarbonyl compounds to enones possess an acidic site, usually the metal center, to activate the enone and a basic site, usually a donor atom of the ligand, which deprotonates the β -keto ester to the enolate to allow for C–C bond formation. Therefore, such catalysts are dubbed “bifunctional”.^{3,4,27} In some examples, the basic site plays a dual role, as it assists the deprotonation of the β -keto ester and its protonated form interacts via a hydrogen bond with the carbonyl oxygen of the enone^{27a,b} or of the enolate.^{3,4} Although our ruthenium/PNNP system apparently does not fit in this class of catalysts, we considered the possibility that the ruthenium-bound carbonyl oxygen of the β -keto ester might behave as such a basic site. Therefore, we explored the hypothesis that a ruthenium-bound enol is formed by a prototropic rearrangement in which the acidic proton is transferred to the ruthenium-bound oxygen atom of the β -carbonyl group. To assess this point further, and in view of the huge uncertainty of the p*K*_a value of Ph₃PH⁺ used as reference in a previous study,¹⁰ we extended our proton transfer studies.

The Acidity of 2a: A Reinvestigation. The estimated aqueous²⁰ p*K*_a of **2a** was determined in CD₂Cl₂ by deprotonation with diphenylamine, whose basicity is reliably defined and in the appropriate range (p*K*_a(Ph₂NH₂⁺) = 0.78).²⁸ The deprotonation of **2a** with Ph₂NH and the protonation of enolato complex **3a** with (Ph₂NH₂)BF₄ gave the same equilibrium position in independent experiments (Scheme 5). In the reaction of the dicationic complex **2a** with Ph₂NH, the resolved signals of **2a** and **3a** (the latter in a small amount) were observed at equilibrium, and the **2a**:**3a** ratio was determined by integration of the inverse-gate-decoupled ³¹P{¹H} NMR spectrum of the reaction solution. Upon protonation of **3a** with (Ph₂NH₂)BF₄, instead of resolved signals, an averaged ³¹P NMR spectrum was

(26) The p*K*_a^{aq} of protonated methyl vinyl ketone is estimated to be approximately –4, as a p*K*_a^{aq} value of –2.87 (on the aqueous scale) has been assigned to protonated 3-methyl-3-penten-2-one,^{26a} and methyl vinyl ketone has been found to be less basic than 3-methyl-3-penten-2-one on the HB scale by about 1.2 p*K* units.^{26b} (a) Levi, A.; Modena, G.; Scorrano, G. *J. Am. Chem. Soc.* **1974**, *96*, 6585. (b) Jensen, J. L.; Thibeault, A. T. *J. Org. Chem.* **1977**, *42*, 2168.

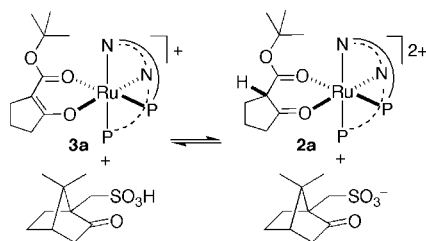
(27) (a) Brunner, H.; Hammer, B. *Angew. Chem., Int. Ed. Engl.* **1984**, *23*, 4–312. (b) Desimoni, G.; Quadrelli, P.; Righetti, P. P. *Tetrahedron* **1990**, *46*, 8–2927. (c) Sasai, H.; Arai, T.; Satow, Y.; Houk, K. N.; Shibasaki, M. *J. Am. Chem. Soc.* **1995**, *117* (23), 6194. (d) Arai, T.; Sasai, H.; Aoe, K.; Okamura, K.; Date, T.; Shibasaki, M. *Angew. Chem., Int. Ed. Engl.* **1996**, *35* (1), 104. (e) Kim, Y. S.; Matsunaga, S.; Das, J.; Sekine, A.; Ohshima, T.; Shibasaki, M. *J. Am. Chem. Soc.* **2000**, *122* (27), 6506.

(28) Dolman, D.; Stewart, R. *Can. J. Chem.* **1967**, *45*, 903.

(24) We estimate a p*K*_a value of ~20 for ketone **8a** on the basis of the aqueous p*K*_a^{aq} of 19 reported for acetone, see: Guthrie, J. P.; Cossar, J.; Klym, A. *J. Am. Chem. Soc.* **1984**, *106*, 1351.

(25) Perrin, D. D. In *Dissociation Constants of Organic Bases in Aqueous Solution: Supplement*; IUPAC: London, 1972.

Scheme 6



observed, which apparently results from fast chemical exchange between **2a** and **3a**. The chemical shift of the high-frequency doublet is close to that of **2a** and was used to determine the **2a**:**3a** ratio.

Averaging all independent data gives a $\text{p}K_{\text{a}}^{\text{aq}}$ of 3.3 ± 0.3 . This value fits nicely into the $\text{p}K_{\text{a}}$ range of 2–5 previously obtained by taking into consideration different $\text{p}K_{\text{a}}$ values for the reference Ph_3PH^+ .¹⁰ We conclude that the coordination to the dicationic Ru/PNNP fragment enhances the acidity of β -keto ester **4a**, which has an estimated $\text{p}K_{\text{a}}^{\text{aq}}$ value of 10.5,²⁹ by a factor of 10^7 . Accordingly, β -keto esters react with aqueous Fe(III) solutions to give enolato complexes even in the presence of Brønsted acids.²³ Such acidity enhancements seem to be markedly substrate-dependent. Thus, the acidity of α -acetyl-*N*-benzyl- δ -valerolactam (**4h**) increases by about 9–10 orders of magnitude upon coordination in **2h** (see above), whereas a smaller acidity enhancement has been found for acetylacetone (acacH), whose $\text{p}K_{\text{a}}$ has been reported to increase from 8.2 to ca. 2.6 upon coordination in $[\text{Ru}(\text{NH}_3)_4(\text{acacH})]^{2+}$ in aqueous solution.^{12a}

With this $\text{p}K_{\text{a}}$ value for **2a** in our hands, we investigated the protonation of enolato complex **3a** at low temperature with the aim of detecting a tautomeric form of **2a**. If a ruthenium-bound enol complex exists, its formation should be kinetically favored at low temperature, as the protonation of the enolato is expected to be faster at an oxygen than at a carbon atom. Camphorsulfonic acid was chosen to protonate **3a** because it is a strong acid and is soluble in dichloromethane. Unfortunately, the acidic properties of strong oxo acids are poorly defined, and largely diverging $\text{p}K_{\text{a}}$ values have been reported for the closely related methane sulfonic acid, which range from 1.62 to -1.92 .³⁰ On the basis of these values, we expected the closely related camphorsulfonic acid to protonate quantitatively the enolato complex **3a**.

A CD_2Cl_2 solution of enolato complex **3a** was cooled to -90 °C in an NMR tube, and camphorsulfonic acid (1 equiv) was added (Scheme 6). The ^{31}P NMR spectrum of the reaction solution at this temperature showed sharp signals of **3a** and of the dicarbonyl complex **2a** roughly in a 1:1 ratio. The high-frequency doublets are well separated at δ 64.5 (**3a**) and 61.6 (**2a**), whereas the low-frequency doublets are overlapped at δ 52.9. Thus, against expectation, the protonation of **3a** with camphorsulfonic acid is not quantitative. Selective irradiation experiments showed that **2a** and **3a** are slowly exchanging even at -90 °C. This indicates that the system is at equilibrium and that the partial protonation is not caused by slow kinetics at low temperature. Upon stepwise warming of the solution, the high-frequency signals start to broaden around -70 °C and collapse into a broad resonance (δ 63.0) at -40 °C. The

Table 6. Estimated Rate and Equilibrium Constants for the Deprotonation of **2a**^{a,b}

entry	B	solvent	k_1 (s ⁻¹)	k_{-1} (s ⁻¹)	2a : 3a
1	—	CD_2Cl_2	2.6 ± 0.4	28 ± 5	92:8
2	4a	CD_2Cl_2	3	27	90:10
3	—	$\text{CD}_2\text{Cl}_2/\text{Et}_2\text{O}$	2.3 ± 0.8	18 ± 3	89:11
4	4a	$\text{CD}_2\text{Cl}_2/\text{Et}_2\text{O}$	5.5 ± 1.1	38 ± 8	87:13

^a From line width analysis of the ^{31}P NMR spectra (Lorentz lines).

^b From ref 14.

coalescence signal resolves and sharpens into a doublet at an equilibrium chemical shift of δ 63.0 upon further warming to 0 °C, indicating fast exchange at this temperature.

The behavior typical for temperature-dependent chemical exchange was also observed for two sets of signals in the ^1H NMR spectra. The imine doublets ($\text{HC}=\text{N}$) of **2a** and **3a** are separated at -90 °C, coalesce at -40 °C, and appear as a sharp signal at the equilibrium chemical shift of δ 8.8 at 0 °C. An additional pair of broad signals was identified around δ 10 and 4.3, which undergoes exchange at -90 °C. Upon warming, the resonance at δ 4.3 gets broader and disappears into the baseline, whereas the one at δ 10 shifts to lower frequency (δ 5.8 at 0 °C). We assign these signals to the acidic proton exchanging between the sulfonic acid and the α -position of the coordinated β -keto ester in **2a**.

All the described temperature-dependent processes are fully reversible between 0 and -90 °C, as identical spectra were obtained after recooling the solution.³¹ We estimate an exchange rate constant of ca. 900 s^{-1} at the coalescence temperature (-40 °C, see Experimental Section), which shows that proton exchange is too fast—even at low temperature—to detect resolved signals for low-concentration species, such as different tautomers of **2a**. Low-temperature protonation experiments with D_2SO_4 and $\text{HBF}_4 \cdot \text{Et}_2\text{O}$ were not conclusive either and will not be discussed.

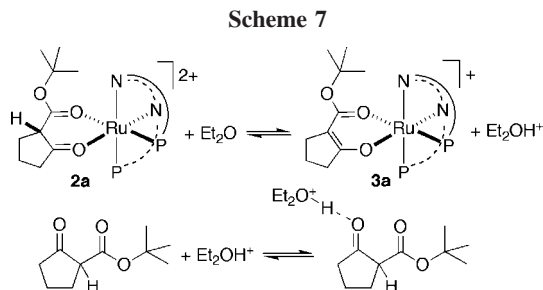
A further problem is that the above result with camphorsulfonic acid is scarcely compatible with the $\text{p}K_{\text{a}}$ value of ca. 3 obtained for **2a** with phosphorus (PPh_3) and nitrogen (Ph_2NH) bases. However, we have recently observed a similar deviation from the expected acid behavior of **2a** in a study of Ru/PNNP-catalyzed fluorination¹⁴ when oxygen donors are present in solution. Thus, when prepared under ether- and acid-free conditions by double chloride abstraction from **1** by TIPF_6 (2 equiv) in the presence of β -keto ester **4a** (1 equiv), **2a** was found to exist in equilibrium with the enolato complex **3a**.³² The base involved was not identified but might be either traces of water or the small amount of β -keto ester **4a** that is set free by the formation of a minor amount of diaqua complex $[\text{Ru}(\text{OH}_2)_2\text{-}(\text{PNNP})]^{2+}$. Selective irradiation and ^{31}P , ^{31}P NOESY exchange NMR spectroscopic experiments indicated that **2a** and **3a** are slowly exchanging at room temperature in CD_2Cl_2 (Table 6,

(31) However, the ^{31}P NMR spectrum of the reaction solution indicates that both **2a** and **3a** decompose at temperatures above 0 °C to unidentified products, probably by replacement of the β -keto ester ligand by the sulfonate anion.

(32) At concentrations above 0.04 M in CD_2Cl_2 . The product ratio is calculated by integration of the ^{31}P NMR spectrum of the reaction solution. When $(\text{Et}_3\text{O})\text{PF}_6$ is used to synthesize **2a** from **1**, no detectable amount of **3a** is observed by NMR spectroscopy, probably because Et_3O^+ reacts with traces of water to give Et_2OH^+ .

(29) As reported for 2-ethoxycarbonylcyclopentanone: Pearson, R. G.; Dillon, R. L. *J. Am. Chem. Soc.* **1953**, *75*, 2439.

(30) (a) Bordwell, F. G.; Algrim, D. *J. Org. Chem.* **1976**, *41*, 2507. (b) Furukawa, N.; Fujihara, H. In *The Chemistry of Sulphonic Acids, Esters, and Their Derivatives*; Patai, S., Rappoport, Z., Eds.; Wiley: Chichester, 1991; pp 261–281.

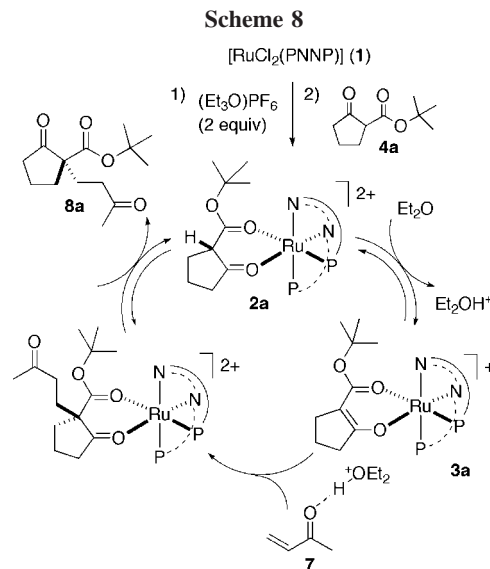


entry 1). The combined addition of β -keto ester **4a** (8 equiv) and of Et_2O to this solution shifts the acid–base equilibrium toward **3a** and accelerates proton exchange (entry 4). This result is unexpected if one considers that the $\text{p}K_{\text{a}}$ of **2a** (3.3) is much higher than the $\text{p}K_{\text{a}}(\text{BH}^+)$ of protonated β -keto ester **4a**, which can reasonably be expected to be between -3 and -4 .^{33,34} Overall, the above results suggest that **2a** behaves as a stronger acid toward oxygen donors than expected on the basis of the $\text{p}K_{\text{a}}$ measurements with phosphorus and nitrogen bases.

In the case of camphorsulfonic acid, we suggest that the low degree of protonation of the enolato complex **3a** observed in CD_2Cl_2 might be related to the inefficient solvation of the conjugate base RSO_3^- in dichloromethane as compared to a protic solvent. Similar arguments have been used to explain the anomalous acid–base behavior of carbonyl compounds (ketones and aliphatic esters).^{33,34} Furthermore, Scorrano and co-workers have shown that the formation of stable hydrogen-bonded adducts between the carbonyl group and H_3O^+ interferes with the protonation equilibrium of ketones and aliphatic esters in aqueous H_2SO_4 solutions.³⁴ This explanation fits nicely our observations concerning the effect of **4a** on the acid–base equilibrium of **2a** (Table 6). Indeed, the deprotonation of **2a** by Et_2O in dichloromethane produces Et_2OH^+ , which can form a strong hydrogen bond with free β -keto ester. We suggest that the formation of the Et_2OH^+ – β -keto ester adduct drives the acid–base equilibrium toward **3a** (Scheme 7). In sum, the above $\text{p}K_{\text{a}}$ data are extremely informative thanks to the common reference to the aqueous scale, as they reveal deviations from the expected behavior, which gives insight into ion pairing, solvation, and other medium effects.

The available pieces of evidence point to the tentative mechanism of the Ru/PNNP-catalyzed Michael addition sketched in Scheme 8, whose key feature is the effect of oxygen donors on the deprotonation of **2a**. As discussed above, the coordination of the β -keto esters to the Ru/PNNP fragment increases the acidity of β -keto ester **4a** by 7 orders of magnitude. We suggest that diethyl ether reinforces this effect under catalytic conditions, in which large excesses of β -keto ester and, more importantly, of methyl vinyl ketone (**7**) are present. As discussed above, **2a** is deprotonated to **3a** in the presence of Et_2O and β -keto ester **4a**. It should be noted that methyl vinyl ketone (**7**) has an estimated $\text{p}K_{\text{a}}$ (ca. -4)^{15,33,34} similar to Et_2OH^+ and protonated **4a** and can, therefore, be protonated or at least be involved in a hydrogen bond, which activates it toward electrophilic attack onto the enolato complex **3a**.

Together with *thermodynamic* acidity, the mobility of the proton on the α -carbon atom, that is, the *kinetic* acidity of **2a**, is enhanced in the presence of oxygen donors. It should be



appreciated that fast deprotonation of the α -position is pivotal for catalysis, as the α -hydrogen on the β -keto ester must be removed before the C–C bond is formed. We observe that the rate of proton transfer is higher in CH_2Cl_2 /ether mixtures than in pure dichloromethane (Table 6), which explains the dramatic effect exerted by oxygen-containing proton shuttles. It should be noted that the tautomerization of the closely related β -diketones is slow even in aqueous solution and is catalyzed by metal ions, in particular by Cu(II), whose catalytic efficiency has been tentatively explained with the formation of a particularly stable complex containing the non-enolized diketone.³⁵

Conclusion

In sum, we have reported rare examples of late transition-metal complexes in which a non-enolized 1,3-dicarbonyl compound is bound to a Lewis-acidic dicationic Ru/PNNP fragment. Upon coordination to ruthenium, the acidity of a 1,3-dicarbonyl compound is enhanced by at least 7 orders of magnitude. In combination with an oxygen-containing co-solvent that acts as a base and a proton shuttle, these complexes efficiently catalyze electrophilic reactions of 1,3-dicarbonyl compounds, including Michael additions and fluorination reactions. We suggest that the role of oxygen-containing co-solvents is to promote (both thermodynamically and kinetically) the deprotonation of the metal-bound β -keto ester, which dramatically enhances the catalytic activity.

Experimental Part

General Procedures. Reactions with air- or moisture-sensitive materials were carried out under an argon atmosphere using Schlenk techniques or in a glovebox. All solvents were distilled from an appropriate drying agent under argon prior to use (CH_2Cl_2 and CD_2Cl_2 from CaH_2 , and hexane from Na/benzophenone). Complex $[\text{RuCl}_2(\text{PNNP})]$ (**1**, PNNP = (1*S*,2*S*)-*N,N'*-bis(*o*-(diphenylphosphino)benzylidene)diaminocyclohexane) was prepared by a literature procedure.³⁶ ^1H , ^{13}C , ^{31}P , and ^{19}F NMR spectra were recorded on Bruker AVANCE spectrometers AC 200, DPX 250, and DPX 300. Multidimensional NMR spectra were recorded on a Bruker AVANCE spectrometer DPX 500. ^1H positive chemical shifts in ppm are downfield from tetramethylsilane. ^{31}P NMR and ^{19}F NMR spectra are referenced to external 85% H_3PO_4 and CFCl_3 , respec-

(33) Lee, D. G.; Sadar, M. H. *J. Am. Chem. Soc.* **1974**, *96*, 2862.

(34) (a) Bagno, A.; Lucchini, V.; Scorrano, G. *J. Phys. Chem.* **1991**, *95*, 345. (b) Bagno, A.; Lucchini, V.; Scorrano, G. *Bull. Soc. Chim. Fr.* **1987**, 563. (c) Bagno, A.; Scorrano, G.; Lucchini, V. *Gazz. Chim. Ital.* **1987**, *117*, 475.

(35) Blanco, C. A.; Hynes, M. J. *Can. J. Chem.* **1991**, *70*, 2285.

(36) Gao, J. X.; Ikariya, T.; Noyori, R. *Organometallics* **1996**, *15*, 1087.

tively. Mass spectra were measured by the MS service of the Laboratorium für Organische Chemie (ETH Zürich). Optical rotations were measured using a Perkin-Elmer 341 polarimeter with a 1 dm cell. Elemental analyses were carried out by the Laboratory of Microelemental Analysis (ETH Zürich). Enantiomeric excesses were determined by HPLC using Agilent HPLC 1100 and HPLC 1050 Series systems.

(1*S*,2*S*)-2-*tert*-Butoxycarbonylcyclopentanone{*N,N'*-bis[2-(diphenylphosphino)benzylidene]diaminocyclohexane}ruthenium(II) Bis(hexafluorophosphate) (2a). Complex **1** (30 mg, 36 μ mol) and (Et₃O)PF₆ (18.3 mg, 74 μ mol, 2.04 equiv) were dissolved in dry CD₂Cl₂ (0.8 mL) in an NMR tube fitted with a Young valve. The resulting solution was stirred at room temperature for 14 h, and then 2-*tert*-butoxycarbonylcyclopentanone (**4a**) (6.5 μ L, 36 μ mol, 1.0 equiv) was added. The NMR spectra of the reaction solution indicated that **2a** was formed in 92% purity (by integration of the ³¹P NMR signals). The characterization of **2a** was carried out on the crude reaction mixture by NMR spectroscopy. ³¹P{¹H} NMR (101 MHz, CD₂Cl₂): δ 61.2 (d, 1 P, $J_{P,P'} = 29.1$ Hz), 51.3 (d, 1 P, $J_{P,P'} = 29.1$ Hz), -144.3 (sept, 2 P, $J_{P,F} = 711$ Hz, PF₆). ¹H NMR (250 MHz, CD₂Cl₂): δ 9.03 (d, 1 H, $J_{P,H} = 9.0$ Hz, $H^bC=N$), 8.83 (s, 1 H, $H^bC=N$), 7.94 (dd, 1 H, $J_{H,H} = 7.2$, 3.2 Hz, benzylidene- H^c), 7.89 (dd, 1 H, $J_{H,H} = 7.4$, 4.3 Hz, H^c), 7.8 – 6.8 (m, 25 H, arom.), 6.72 (dd, 1 H, $J_{H,H} = 8.8$, 8.8 Hz, arom.), 3.78 (dd, 1 H, $J_{H,H} = 11.0$, 9.1 Hz, C(O)CH^dCOO), 3.40–3.32 (m, 1 H, H^aC-N), 3.00 (br d, 1 H, $J_{H,H} = 11.4$ Hz, CHH'), 2.52–2.42 (m, 2 H, CH₂), 2.42–2.35 (m, 1 H, H^aC-N), 1.96 (br d, 1 H, $J_{H,H} = 13.6$ Hz, CHH'), 1.92–1.83 (m, 1 H, CHH'), 1.67–1.62 (m, 2 H, CH₂), 1.46–1.37 (m, 1 H, CHH'), 1.36–1.25 (m, 3 H, CHH'), 1.25–1.16 (m, 1 H, CHH'), 1.21 (s, 9 H, C(CH₃)₃), 1.00–0.90 (m, 1 H, CHH'), 0.82–0.71 (m, 1 H, CHH'). ¹³C{¹H} NMR (126 MHz, CD₂Cl₂): δ 227.3 (C=O), 175.2 (COO), 170.9 (d, $J_{C,P} = 4.8$ Hz, C=N), 168.6 (d, $J_{C,P} = 4.9$ Hz, C=N), 139.6–125.5 (36 C, arom.), 90.8 (OC(CH₃)₃), 78.0 (C ^{α} -N), 70.0 (C ^{α} -N), 55.5 (C(O)CH^dCOO), 32.2 (CH₂), 31.5 (CH₂), 28.1 (C(O)CH₂CH₂CH₂), 27.9 (C(CH₃)₃), 27.2 (CH₂), 24.9 (CH₂), 24.1 (CH₂), 19.5 (CH₂).

(1*S*,2*S*)-2-*tert*-Butoxycarbonylcyclopentanoato{*N,N'*-bis[2-(diphenylphosphino)benzylidene]diaminocyclohexane}ruthenium(II) Hexafluorophosphate (3a). A solution of **1** (80 mg, 96 μ mol) and (Et₃O)PF₆ (49 mg, 197 μ mol, 2.05 equiv) in CH₂Cl₂ (5 mL) was stirred at room temperature for 16 h. Then, 2-*tert*-butoxycarbonylcyclopentanone (**4a**) (20 mg, 109 μ mol, 1.13 equiv) in CH₂Cl₂ (1 mL) was added, and the resulting solution was stirred for 1 h at room temperature. After adding triethylamine (15 μ L, 108 μ mol, 1.13 equiv) and stirring for a further 45 min, the crude reaction mixture was filtered through a short plug of silica gel with dichloromethane as eluent. After evaporation of the solvent, the orange product was triturated with hexane and dried under vacuum. The analytically pure product was obtained as an orange solid. Yield: 67 mg (61.6 μ mol, 64%). ³¹P{¹H} NMR (101 MHz, CD₂Cl₂): δ 63.4 (d, 1 P, $J_{P,P'} = 31.2$ Hz), 52.5 (d, 1 P, $J_{P,P'} = 31.2$ Hz), -144.3 (sept, 1 P, $J_{P,F} = 711$ Hz, PF₆). ¹H NMR (500 MHz, CD₂Cl₂): δ 8.89 (s, 1 H, $H^bC=N$), 8.69 (d, 1 H, $J_{P,H} = 9.5$ Hz, $H^bC=N$), 7.79 (dd, 1 H, $J_{H,H} = 7.2$, 4.1 Hz, H^c), 7.66–7.58 (m, 4 H, arom.), 7.53–7.48 (m, 3 H, arom.), 7.46–7.34 (m, 7 H, arom.), 7.21–7.15 (m, 6 H, arom.), 7.03–6.90 (m, 4 H, arom.), 6.89 (ddd, 2 H, $J_{H,H} = 7.6$, 7.6, 1.8 Hz, arom.), 6.52 (dd, 1 H, $J_{H,H} = 8.7$, 8.7 Hz, arom.), 3.80–3.71 (m, 1 H, H^aC-N), 2.58–2.50 (m, 1 H, CHH'), 2.43–2.35 (m, 1 H, CHH'), 2.30–2.21 (m, 1 H, H^aC-N), 2.04 (ddd, 1 H, $J_{H,H} = 13.3$, 7.6, 6.1 Hz, CHH'), 1.98–1.86 (m, 2 H, CH₂), 1.77–1.66 (m, 2 H, CH₂), 1.62–1.53 (m, 1 H, CHH'), 1.33–1.22 (m, 3 H, CHH'), 1.21–1.13 (m, 3 H, CHH'), 1.11 (s, 9 H, C(CH₃)₃). ¹³C{¹H} NMR (126 MHz, CD₂Cl₂): δ 192.0 (C=C-O), 168.3 (COO), 166.7 (d, $J_{C,P} = 3.1$ Hz, C=N), 163.5 (d, $J_{C,P} = 5.2$ Hz, C=N), 138.2–126.4 (36 C, arom.), 93.1 (C=C-O), 79.4 (OC(CH₃)₃), 78.2 (C-N), 68.7 (C-N), 38.9 (CH₂), 32.2 (CH₂), 31.9 (CH₂), 29.3 (C(CH₃)₃), 28.8 (CH₂), 25.0 (CH₂),

24.2 (CH₂), 20.2 (CH₂). Anal. Calcd for C₅₄H₅₅F₆N₂O₃P₃Ru (1088.0): C 59.61, H 5.09, N 2.57. Found: C 59.86, H 5.20, N 2.54.

(1*S*,2*S*)- α -Acetyl-*N*-benzyl- δ -valerolactam{*N,N'*-bis[2-(diphenylphosphino)benzylidene]diaminocyclohexane}ruthenium(II) Bis(hexafluorophosphate) (2h). A solution of (Et₃O)PF₆ (120 mg, 0.48 mmol, 2.0 equiv) in CH₂Cl₂ (2 mL) was added to **1** (200 mg, 0.24 mmol) in CH₂Cl₂ (3 mL), and the resulting solution was stirred for 6 h. α -Acetyl-*N*-benzyl- δ -valerolactam (**4h**) (60 mg, 0.26 mmol, 1.1 equiv) in CH₂Cl₂ (2 mL) was added to the solution, whose color turned from deep brown to orange. After stirring for 12 h, the solvent was evaporated under reduced pressure, and the yellow solid was washed with hexane. Yield: 280 mg (91%). ³¹P{¹H} NMR (101 MHz, CD₂Cl₂): δ 60.7 (d, 1 P, $J_{P,P'} = 28.9$ Hz), 50.5 (d, 1 P, $J_{P,P'} = 28.9$ Hz), -144.3 (sept, 2 P, $J_{P,F} = 711$ Hz, PF₆). ¹H NMR (500 MHz, CD₂Cl₂): δ 8.90 (d, 1 H, $J_{P,H} = 9.5$ Hz, $H^bC=N$), 8.36 (s, 1 H, $H^bC=N$), 8.05 – 8.00 (m, 1 H, benzylidene- H^c), 7.95–6.70 (m, 29 H, arom.), 6.83 (d, 2 H, $J_{H,H} = 7.46$ Hz, *ortho*-NBn- H^b), 6.66–6.57 (m, 1 H, arom.), 4.19 (d, 1 H, $J_{H,H} = 15.5$ Hz, NCH ^{β} H ^{β} Ph), 3.75 (d, 1 H, $J_{H,H} = 15.5$ Hz, NCH ^{β} H ^{β} Ph), 3.63 (dd, 1 H, $J_{H,H} = 11.0$, 5.5 Hz, C(O)CH^dC(O)N), 3.45–3.40 (m, 1 H, NCHH'CH₂), 3.35–3.26 (m, 1 H, NCHH'CH₂), 2.79–2.73 (m, 1 H, CHH'), 2.73–2.65 (m, 1 H, H^aC-N), 2.27–2.13 (m, 1 H, CHH'), 2.03–1.95 (m, 2 H, CH₂), 1.97–1.88 (m, 1 H, H^aC-N), 1.89–1.83 (m, 2 H, CH₂), 1.77–1.68 (m, 2 H, CH₂), 1.32–1.21 (m, 2 H, CH₂), 1.59 (s, 3 H, CH₃), 0.92–0.82 (m, 1 H, CHH'), 0.83–0.71 (m, 1 H, CHH'). ¹³C{¹H} NMR (176 MHz, CD₂Cl₂): δ 218.8 (CH₃C^dO), 169.2 (d, $J_{C,P} = 5.0$ Hz, C=N), 167.4 (d, $J_{C,P} = 5.0$ Hz, C=N), 167.2 (C ^{α} (O)-N), 139.0–125.4 (42 C, arom.), 78.0 (C ^{α} -N), 69.4 (C ^{α} -N), 53.5 (NCH₂Ph), 50.9 (NCH₂CH₂), 50.5 (C(O)CH^dC(O)N), 31.4 (CH₂), 31.2 (CH₂), 31.2 (CH₂), 25.0 (NCH₂CH₂C^dH₂), 24.7 (CH₂), 23.4 (CH₂), 20.6 (CH₂). ¹⁹F NMR (188 MHz, CD₂Cl₂): δ -72.5 (d, 12 F, $J_{F,P} = 712$ Hz, PF₆). MS (MALDI): m/z 990 (M⁺ (-H⁺), 61), 759 (M⁺ - **4b**, 100), 573 (M⁺ - **4b** - 2PPh₂, 10). Anal. Calcd for C₅₈H₅₇F₁₂N₃O₂P₄Ru: C, 54.38; H, 4.48; N, 3.28. Found: C, 54.73; H, 4.87; N, 3.07.

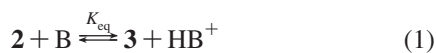
(1*S*,2*S*)- α -Acetyl-*N*-benzyl- δ -valerolactamato{*N,N'*-bis[2-(diphenylphosphino)benzylidene]diaminocyclohexane}ruthenium(II) Hexafluorophosphate (3h). A solution of (Et₃O)PF₆ (64 mg, 0.255 mmol, 2.0 equiv) in CH₂Cl₂ (2 mL) was added to **1** (106 mg, 0.127 mmol) in CH₂Cl₂ (3 mL), and the resulting solution was stirred for 6 h. α -Acetyl-*N*-benzyl- δ -valerolactam (**4h**) (29 mg, 0.127 mmol, 1.0 equiv) in CH₂Cl₂ (2 mL) was added to the solution, whose color turned from deep brown to orange. After stirring the solution for 2 h, triethylamine was added (0.018 mL, 0.129 mmol, 1.02 equiv). The solution color turned instantaneously to red. The solvent was evaporated after 1 h under reduced pressure, and the red solid was washed with hexane. Flash chromatography on silica gel (CH₂Cl₂) afforded the product as a red crystalline solid. Yield: 80 mg (55%). ³¹P{¹H} NMR (121 MHz, CD₂Cl₂): δ 61.5 (d, 1 P, $J_{P,P'} = 30.4$ Hz), 51.9 (d, 1 P, $J_{P,P'} = 30.4$ Hz), -144.3 (sept, 1 P, $J_{P,F} = 711$ Hz, PF₆). ¹H NMR (300 MHz, CD₂Cl₂): δ 8.56 (s, 1 H, $H^bC=N$), 8.54 (d, 1 H, $J_{P,H} = 11.7$ Hz, $H^bC=N$), 7.75–7.67 (m, 1 H, H^c), 7.67–6.83 (m, 30 H, arom.), 6.90 (d, 1 H, $J_{H,H} = 8.1$ Hz, *ortho*-NBn- H^b), 6.51 (dd, 1 H, $J_{H,H} = 8.6$, 8.6 Hz, arom.), 4.38 (d, 1 H, $J_{H,H} = 16.1$ Hz, NCH ^{β} H ^{β} Ph), 3.44 (d, 1 H, $J_{H,H} = 16.1$ Hz, NCH ^{β} H ^{β} Ph), 3.20 – 3.05 (m, 1 H, H^aC-N), 3.15–3.06 (m, 1 H, NCHH'CH₂), 3.00–2.90 (m, 1 H, NCHH'CH₂), 2.30–2.20 (m, 1 H, CHH'), 2.1–1.9 (m, 2 H, CH₂), 2.00–1.88 (m, 1 H, H^aC-N), 1.83–1.71 (m, 1 H, CHH'), 1.70–1.52 (m, 4 H, CH₂), 1.15 (s, 3 H, CH₃), 1.08–0.93 (m, 1 H, CH₂), 0.96–0.82 (m, 1 H, CH₂), 0.77–0.59 (m, 2 H, CH₂). ¹³C{¹H} NMR (176 MHz, CD₂Cl₂): δ 178.3 (CH₃C(O)=C), 164.9 (C=N), 163.1 (CO-N), 161.6 (d, $J_{C,P} = 5.3$ Hz, C=N), 139.1–124.8 (42 C, arom.), 89.0 (CH₃C(O)=C), 77.9 (C-N), 68.1 (C-N), 51.2 (NCH₂Ph), 49.1 (NCH₂CH₂), 31.1 (CH₂), 30.9 (CH₂), 26.5 (CH₂), 25.6 (CH₃), 24.4 (CH₂), 23.0 (CH₂), 22.7 (CH₂). ¹⁹F NMR (188 MHz, CD₂Cl₂): δ

−73.4 (d, 12 F, $J_{\text{F,P}} = 712$ Hz, PF_6). MS (ESI): m/z 990 (M^+ , 100), 759 ($\text{M}^+ - \text{enolato}$, 5), 573 ($\text{M}^+ - \text{enolato} - 2\text{PPh}_2$, 10). Anal. Calcd for $\text{C}_{58}\text{H}_{56}\text{F}_6\text{N}_3\text{O}_2\text{P}_3\text{Ru}$: C, 61.37; H, 4.97; N, 3.70. Found: C, 61.96; H, 5.00; N, 3.52.

Diphenylammonium Tetrafluoroborate. HBF_4 in Et_2O (54 wt %, 1.6 mL, 11.9 mmol, 1.0 equiv) was added to a solution of diphenylamine (2.0 g, 11.8 mmol) in Et_2O (10 mL) at 0 °C under an argon atmosphere. A white solid precipitated, which was collected by filtration under argon, washed twice with Et_2O (10 mL each), and dried under vacuum. Yield: 2.756 g (10.7 mmol, 91%). ^1H NMR (250.1 MHz, CD_2Cl_2): δ 9.7 (br s, 2 H, Ph_2NH_2^+), 7.53 (br s, 10 H, arom. H).

Pyridinium Tetrafluoroborate. To a Et_2O solution (5 mL) of pyridine (1 mL, 12.4 mmol), cooled to 0 °C, was added a solution of HBF_4 in Et_2O (54 wt %, 2 mL, 14.5 mmol, 1.2 equiv), which gave a white precipitate. After the mixture was allowed to reach room temperature, the solid was collected by filtration, washed twice with Et_2O , and dried under vacuum. Yield: 1.98 g (96%). ^1H NMR (250 MHz, DMSO): δ 8.97–8.78 (m, 2H, ArH), 8.68–8.50 (m, 1H, ArH), 8.20–7.92 (m, 2H, ArH), 7.09 (s, 1H, NH).

Estimation of the $\text{p}K_{\text{a}}$. The estimated aqueous $\text{p}K_{\text{a}}$ values²⁰ of **2a** and **3h** were determined from the position of the deprotonation equilibrium (eq 1) with an appropriate base (B) by combining K_{eq} with the $\text{p}K_{\text{a}}$ value of B (eqs 2, 3). When resolved signals for **2** and **3** were observed, K_{eq} was calculated from the integrated intensities of the signals of **2a** and **3a** in the $^{31}\text{P}\{\text{inverse-gated}^1\text{H}\}$ NMR spectra with the assumption that $[\mathbf{3}] = [\text{BH}^+]$ and $[\mathbf{2}] = [\text{B}]$. In the case of a fast proton exchange, the ^{31}P NMR spectrum exhibited a single coalescence signal at δ_{eq} (the weighted average of chemical shifts of **2** and **3**), from which the $[\mathbf{3a}]/[\mathbf{2a}]$ ratio was calculated with eq 5, where δ_2 and δ_3 are the chemical shifts of complexes **2** and **3**, respectively. Numeric values for the integrated intensities and for the chemical shifts were obtained by using both the Fourier-transformed spectrum and a Lorentzian fit. All reaction solutions were analyzed by $^{31}\text{P}\{\text{inverse-gated}^1\text{H}\}$ NMR spectroscopy.



$$K_{\text{eq}} = \frac{[\mathbf{3}][\text{HB}^+]}{[\mathbf{2}][\text{B}]} \quad (2)$$

$$\text{p}K_{\text{a}}(\mathbf{2}) = \text{p}K_{\text{eq}} + \text{p}K_{\text{a}}^{\text{aq}}(\text{B}) \quad (3)$$

$$K_{\text{eq}} \cong \left(\frac{[\mathbf{3}]}{[\mathbf{2}]} \right)^2 \quad (4)$$

$$\frac{[\mathbf{3}]}{[\mathbf{2}]} = \frac{\delta_{\text{eq}} - \delta_2}{\delta_3 - \delta_{\text{eq}}} \quad (5)$$

Acidity of 2a. The position of equilibrium 1 was independently determined by deprotonation of **2a** with Ph_2NH and in the protonation of **3a** with $(\text{Ph}_2\text{NH}_2)\text{BF}_4$. Complex **2a** was prepared by stirring a mixture of **1** (20 mg, 24.1 μmol), TIPF_6 (20 mg, 57.3 μmol , 2.4 equiv), and 2-*tert*-butoxycarbonylcyclopentanone (**4a**) (4.4 μL , 24.3 μmol , 1.0 equiv) in CD_2Cl_2 (0.6 mL) at room temperature for 15 h. After filtration, diphenylamine (4.1 mg, 24.2 μmol , 1.0 equiv) was added, and the solution was analyzed by ^{31}P NMR spectroscopy. Separate signals of **2a** and **3a** were obtained, whose integrals were used in the approximation of eq 4. Fourier spectrum: $[\mathbf{3a}]/[\mathbf{2a}] = 0.054$, Lorentzian line fit: $[\mathbf{3a}]/[\mathbf{2a}] = 0.087$. For the protonation reaction, **3a** (26 mg, 23.9 μmol) and $(\text{Ph}_2\text{NH}_2)\text{BF}_4$ (6.2 mg, 24.1 μmol , 1.0 equiv) were dissolved in CD_2Cl_2 (0.6 mL), and the reaction mixture was analyzed by ^{31}P NMR spectroscopy. The high-frequency doublet of **2a** appeared at an equilibrium chemical shift of δ_{eq} 61.30, which was used to calculate the $[\mathbf{3a}]/[\mathbf{2a}]$ ratio with eq 5. Fourier spectrum: $[\mathbf{3a}]/[\mathbf{2a}]$

$= 0.040$, Lorentzian line fit: $[\mathbf{3a}]/[\mathbf{2a}] = 0.038$. The deprotonation of **2a** and the protonation of **3a** gave the same K_{eq} value. Averaging all data from both the deprotonation and the protonation experiment gives an estimated aqueous $\text{p}K_{\text{a}}$ of 3.3 ± 0.3 for **2a** (with $\text{p}K_{\text{a}}^{\text{aq}} = 0.78$ as reference for Ph_2NH_2^+).²⁸

Acidity of 2h. The $\text{p}K_{\text{a}}$ of **2h** was measured against pyridine with the approximation of eq 4 because the ^1H NMR signal of the pyridinium ion overlaps with signals of the PNNP ligand. Complex **2h** (16 mg, 12.5 μmol) was dissolved in CD_2Cl_2 (0.5 mL). A CD_2Cl_2 solution of pyridine (125 μL , 0.1 M, 12.5 μmol) was added. The reaction mixture was stirred for 1 h, then transferred into an NMR tube and analyzed by ^{31}P NMR spectroscopy. In the inverse reaction, **3h** (20 mg, 17.6 μmol) was dissolved in CD_2Cl_2 (0.5 mL), and pyridinium tetrafluoroborate (3.0 mg, 17.6 μmol) was added. After stirring for 1 h, the solution was transferred into an NMR tube and analyzed. Both the deprotonation of **2h** and the protonation of **3h** gave resolved ^{31}P NMR signals of **2h** and **3h**. Averaging all the independent data from eq 4 yields an estimated aqueous $\text{p}K_{\text{a}}$ value²⁰ of 4.67 ± 0.08 (with $\text{p}K_{\text{a}}^{\text{aq}} = 5.14$ for pyridine as reference).³⁷

Catalytic Michael Addition Reactions. Complex **1** (30 mg, 36 μmol , 5 mol %) and $(\text{Et}_3\text{O})\text{PF}_6$ (19 mg, 76 μmol , 2 equiv, 10 mol %) (or the corresponding halide scavenger) were dissolved in CH_2Cl_2 (2 mL), and the solution was stirred for 16 h. After the activation with oxonium salts, the β -keto ester **4a** (133 mg, 0.722 mmol) (or the corresponding substrate) and decane (100 mg, as GC internal standard) were added directly to the catalyst solution. Upon activation with Ag(I) salts, the slurry was filtered over Celite before adding the substrates. After adding methyl vinyl ketone (**7**) (71.0 mL, 86.4 mmol, 1.2 equiv), the solution was stirred for 24 h at room temperature and then analyzed by quantitative GC analysis (with decane as internal standard) to determine substrate conversion and product yield. To enhance the reproducibility of the yield determination by GC analysis, the sample was treated with an excess of $(\text{Et}_4\text{N})\text{Cl}$ to displace the coordinated Michael product **8** from ruthenium.³⁸ The products were isolated, purified, and characterized as described below.

***tert*-Butyl 2-Oxo-1-(3-oxobutyl)cyclopentanecarboxylate (8a).** R_f (silica gel 60, hexane/TBME, 4:1) = 0.2. ^1H NMR (200 MHz, CDCl_3): δ 2.88–2.20 (m, 6H, CH_2), 2.17 (s, 3 H, $\text{C}(\text{O})\text{CH}_3$), 2.11–1.80 (m, 4H, CH_2), 1.47 (s, 9H, $3 \times \text{C}(\text{O})\text{OCH}_3$). $^{13}\text{C}\{^1\text{H}\}$ NMR (125.7 MHz, CDCl_3): δ 251.5 (C^2), 208.3 ($\text{C}(\text{O})\text{CH}_3$), 171.0 ($\text{C}(\text{O})\text{O}^t\text{Bu}$), 82.3 ($\text{C}(\text{O})\text{OC}(\text{CH}_3)_3$), 59.8 (C^1), 39.2 ($\text{CH}_2\text{C}(\text{O})\text{CH}_3$), 38.3 (C^3H_2), 34.8 ($\text{CH}_2\text{CH}_2\text{C}(\text{O})\text{CH}_3$), 30.2 ($\text{C}(\text{O})\text{CH}_3$), 28.2 ($\text{C}(\text{O})\text{OC}(\text{CH}_3)_3$), 27.4 (C^5H_2), 19.9 (C^4H_2). GC-MS (50 °C (3 min) to 250 °C (10 min) at 8 °C/min): $t_R = 19.69$ min, m/z 198.00 (60, $[\text{M}^+ - \text{C}_4\text{H}_8]$). HPLC (Daicel CHIRALPACK AS, 0.5 mL/min, hexane/*i*-PrOH, 99:1): $t_R = 26.15$ min (*R* enantiomer); 32.3 min (*S* enantiomer). The absolute configuration was assigned by comparison of HPLC data and sign of the optical rotation to literature data.^{6a} $[\alpha]^{25}\text{D} @ 79\% \text{ ee} = +5.954(5)$ (CHCl_3 , $c = 2.7$). MS (EI): m/z 254.15 (3, $[\text{M}]^+$), 226.16 (12, $[\text{M} - \text{C}_2\text{H}_4]^+$), 198.09 (26, $[\text{M} - t\text{-Bu}]^+$), 170.10 (54, $[\text{M} - \text{C}_2\text{H}_4 - t\text{-Bu}]^+$), 137.10 (30), 97.07 (34), 57.07 (100, $[t\text{-Bu}]^+$), 43.02 (72, $[\text{C}_2\text{H}_3\text{O}]^+$). Analytical data are consistent with literature data.^{6a}

Ethyl 2-Oxo-1-(3-oxobutyl)cyclopentanecarboxylate (8b). R_f (silica gel 60, hexane/TBME, 4:1) = 0.2. ^1H NMR (250 MHz, CDCl_3): δ 3.82 (q, 2H, $J_{\text{H,H}} = 7$ Hz, $\text{C}(\text{O})\text{OCH}_2\text{CH}_3$), 2.45–2.25 (m, 1H, CHH'), 2.20–1.84 (m, 4H, $2 \times \text{CH}_2$), 1.84–1.40 (m, 5H, $2 \times \text{CH}_2 + \text{CHH}'$), 1.79 (s, 3H, $\text{C}(\text{O})\text{OCH}_2\text{CH}_3$), 0.91 (*t*, $J_{\text{H,H}} = 7$ Hz, 3H, $\text{C}(\text{O})\text{CH}_3$). $^{13}\text{C}\{^1\text{H}\}$ NMR (75.5 MHz, CDCl_3): δ 214.9 (C^2), 207.8 ($\text{C}(\text{O})\text{CH}_3$), 171.3 ($\text{C}(\text{O})\text{OEt}$), 61.4 ($\text{C}(\text{O})\text{OCH}_2\text{CH}_3$),

(37) Brown, H. C.; McDaniel, D. H.; Häffiger, O. In *Determination of Organic Structures by Physical Methods*; Braude, E. A., Nachod, F. C., Eds.; Academic Press: New York, 1955.

(38) In the Ru/PNNP-catalyzed fluorination of β -keto esters, we have observed that the fluorinated β -keto ester remains coordinated to ruthenium, although it binds more weakly to ruthenium than the substrate **4a**.¹⁴

58.9 (C^1), 38.8 ($CH_2C(O)CH_3$), 37.9 (C^3H_2), 34.2 ($CH_2CH_2C(O)CH_3$), 29.8 ($C(O)CH_3$), 26.9 (C^5H_2), 19.5 (C^4H_2), 14.0 ($C(O)OCH_2CH_3$). HPLC (Daicel CHIRALPACK AS, 0.5 mL/min, hexane/*i*-PrOH, 99:1): $t_R = 42.0$ min, minor; 44.5 min, major. GC-MS (50 °C (3') to 250 °C (10') at 8 °C/min): $t_R = 19.04$ min, m/z 227.06 (0.4, $[M + H]^+$), m/z 198.03 (55, $[M - C_2H_4]^+$), m/z 180.02 (40, $[M - EtOH]^+$). Analytical data are consistent with literature data.^{6a}

Benzyl 2-Oxo-1-(3-oxobutyl)cyclopentanecarboxylate (8c). R_f (silica gel 60, hexane/TBME, 2:1) = 0.2. 1H NMR (300 MHz, $CDCl_3$): δ 7.40–7.25 (m, 5H, PhH), 5.13 (app s, 2H, CH_2Ph), 2.71–2.56 (m, 1H, $CHH'C(O)CH_3$), 2.48–2.33 (m, 1H, $CHH''C(O)CH_3$), 2.51–2.38 (m, 1H, $CHH'CH_2C(O)CH_3$), 1.93–1.78 (m, 1H, $CHH''CH_2C(O)CH_3$), 2.45–2.12 (m, 2H, C^3H_2), 2.05 (s, 3H, $C(O)CH_3$), 2.21–2.07 (m, 1H, C^5HH'), 1.98–1.84 (m, 1H, C^5HH''), 2.20–1.95 (m, 1H, C^4HH'), 2.02–1.87 (m, 1H, C^4HH''). $^{13}C\{^1H\}$ NMR (75.5 MHz, $CDCl_3$): δ 214.5 (C^2), 207.6 ($C(O)CH_3$), 171.1 ($C(O)OBz$), 135.5 (*ipso*-arom), 128.6 (2C, *meta*-arom), 128.3 (2C, *ortho*-arom), 128.0 (*para*-arom), 67.0 ($C(O)OCH_2Ph$), 59.0 (C^1), 38.7 ($CH_2C(O)CH_3$), 38.0 (C^5H_2), 34.2 ($CH_2CH_2C(O)CH_3$), 29.8 ($C(O)CH_3$), 27.0 (C^5H_2), 19.5 (C^4H_2). HPLC (Daicel CHIRALPACK OJ, 0.5 mL/min, hexane/*i*-PrOH, 90:10): $t_R = 62.5$ min (major), 70.0 min (minor). Analytical data are consistent with the literature data.³⁹

2-Acetyl-2-methyl-5-oxo-hexanoic Acid Ethyl Ester (8d). R_f (silica gel 60, hexane/TBME, 4:1) = 0.3. 1H NMR (300 MHz, $CDCl_3$): δ 4.08 (q, $J_{H,H} = 7.2$ Hz, 2H, $C(O)OCH_2CH_3$), 2.41–2.23 (m, 2H, $C^4H_2C(O)CH_3$), 2.10–1.88 (m, 2H, C^3H_2), 2.05 (s, 3H, $C^2(Me)C(O)CH_3$), 2.03 (s, 3H, $C(O)C^6H_3$), 1.23 (s, 3H, $CH_3C(O)C(CH_3)C(O)OEt$), 1.16 (t, $J_{H,H} = 7.2$ Hz, 3H, $C(O)OCH_2CH_3$). $^{13}C\{^1H\}$ NMR (75.5 MHz, $CDCl_3$): δ 207.2 (C^5), 205.2 ($C(O)CH_3$), 172.5 ($C(O)OEt$), 61.3 ($C(O)OCH_2CH_3$), 58.5 ($CH_3C(O)C^2(Me)C(O)OEt$), 38.4 ($C^4H_2C(O)CH_3$), 29.8 ($C(O)C^6H_3$), 28.3 ($C^3H_2CH_2C(O)CH_3$), 26.0 ($C^2(Me)C(O)CH_3$), 19.1 (C^2CH_3), 13.9 ($C(O)OCH_2CH_3$). $[\alpha]_D^{25} + 1.27(4)$ ($CHCl_3$, $c = 1.0$) (10% ee) calculated from the reported value.^{6a} GC-MS (50 °C (3') to 250 °C (10') at 8 °C/min): $t_R = 16.4$ min, m/z 215.08 (1, $[M + H]^+$), 173.13 (26), 171.86 (86), 143.94 (52), 125.28 (100), 114.98 (74), 97.39 (98), 86.89 (76), 68.93 (60), 57.99 (56), 42.82 (90), 29.05 (44). Analytical data are consistent with literature data.^{6a}

2-Acetyl-2-methyl-5-oxo-hexanoic Acid Benzyl Ester (8e). R_f (silica gel 60, hexane/TBME, 4:1) = 0.2. 1H NMR (300 MHz, $CDCl_3$): δ 7.35–7.25 (m, 5H, arom), 5.11 (app s, 2H, CH_2Ph), 2.31–2.20 (m, 2H, C^4H_2), 2.03 (s, 3H, C^6H_3), 2.00 (s, 3H, $C^2C(O)CH_3$), 2.20–1.90 (m, 2H, C^3H_2), 1.29 (s, 3H, C^2CH_3). $^{13}C\{^1H\}$ NMR (75.5 MHz, $CDCl_3$): δ 207.7 ($C^2C(O)CH_3$), 205.8 ($C^5(O)CH_3$), 171.1 (C^1), 136.1 (*ipso*-arom), 128.7 (2C, *meta*-arom), 128.3 (*para*-arom), 128.0 (2C, *ortho*-arom), 66.9 (CH_2Ph), 55.9 (C^2), 38.5 (C^4), 29.8 (C^6), 28.8 (C^3), 20.0 (C^2CH_3). HPLC (Daicel CHIRALPACK OJ, 0.8 mL/min, hexane/*i*-PrOH, 98:2): $t_R = 58.5$ min (minor), 62.7 min (major). Analytical data are consistent with literature data.⁴⁰

2-Benzoyl-2-methyl-5-oxo-hexanoic Acid Ethyl Ester (8f). R_f (silica gel 60, hexane/TBME, 4:1) = 0.15. 1H NMR (300 MHz, $CDCl_3$): δ 7.81 (d, $J_{H,H} = 7.53$ Hz, 2H, *ortho*-arom), 7.51 (t, $J_{H,H} = 7.22$, 1H, *para*-arom), 7.40 (dd, $J_{H,H} = 7.53$, $J_{H,H'} = 7.22$ Hz, 2H, *meta*-arom), 4.100 (q, $J_{H,H} = 7.11$ Hz, 1H, $C^1(O)OCHH'CH_3$), 4.098 (q, $J_{H,H} = 7.11$ Hz, 1H, $C^1(O)OCHH''CH_3$), 2.58–2.18 (m, 4H, $C^3H_2 + C^4H_2$), 2.10 (s, 3H, C^6H_3), 1.47 (s, 3H, C^2CH_3), 1.04 (app t, $J_{H,H} = 7.11$ Hz, 3H, $C^1(O)OCH_2CH_3$). $^{13}C\{^1H\}$ NMR (75 MHz, $CDCl_3$): δ 207.3 (C^5), 197.2 ($C^2C(O)Ph$), 173.9 (C^1), 135.4 (*ipso*-arom), 132.8 (*para*-arom), 128.5 (4C, *ortho* + *meta*-arom), 61.4 ($C^1(O)OCH_2CH_3$), 56.0 (C^2), 38.4 (C^4H_2), 30.1 (C^3H_2), 29.9 (C^6H_3), 21.3 (C^2CH_3), 13.7 ($C^1(O)OCH_2CH_3$). HPLC (Daicel

CHIRALPACK OJ, 0.5 mL/min, hexane/*i*-PrOH, 98:2): $t_R = 52.0$ min (minor), 55.9 min (major).

2-Ethoxycarbonyl-2-(3-oxobutyl)-1-indanone (8g). R_f (silica gel 60, hexane/TBME, 2:1) = 0.2. 1H NMR (500 MHz, C_6D_6): δ 7.88–7.80 (m, 1H, arom), 7.30–7.27 (m, 1H, arom), 7.20–7.15 (m, 1H, arom), 7.10–7.05 (m, 1H, arom), 4.02–3.92 (m, 2H, $C(O)OCH_2CH_3$), 3.56 (d, 1H, $J_{H,H} = 17.3$ Hz, C^3HH'), 2.76 (d, 1H, $J_{H,H} = 17.3$ Hz, C^3HH''), 2.57–2.33 (m, 4H, $CH_2CH_2C(O)CH_3 + CH_2CH_2C(O)CH_3$), 1.74 (s, 3H, $CH_2CH_2C(O)CH_3$), 0.96–0.90 (m, 3H, $C(O)OCH_2CH_3$). $^{13}C\{^1H\}$ NMR (125.8 MHz, C_6D_6): δ 205.79 ($CH_2CH_2C(O)CH_3$), 202.14 (C^1), 171.31 ($C(O)OEt$), 153.03 (arom), 136.06 (arom), 135.34 (arom), 128.18 (arom), 126.78 (arom), 124.99 (arom), 61.58 ($C(O)OCH_2CH_3$), 59.74 (C^2), 38.96 ($CH_2CH_2C(O)CH_3$), 38.06 (C^3), 29.47 ($CH_2CH_2C(O)CH_3$), 29.06 ($CH_2CH_2C(O)CH_3$), 14.12 ($C(O)OCH_2CH_3$). HPLC (Reprosil Chiral NR, 0.8 mL/min, hexane/*i*-PrOH, 95:5): $t_R = 72.9$ min, 76.1 min, racemic. Analytical data are consistent with literature data.⁴¹

3-Acetyl-1-benzyl-3-(3-oxobutyl)piperidin-2-one (8h). R_f (silica gel 60, hexane/TBME, 2:1) = 0.1. 1H NMR (400 MHz, $CDCl_3$): δ 7.38–7.24 (m, 5H, arom), 4.79 (d, 1H, $J_{H,H} = 14.5$ Hz, $CHH'Ph$), 4.43 (d, 1H, $J_{H,H} = 14.5$ Hz, $CHH''Ph$), 3.29–3.21 (m, 2H, C^6H_2), 2.64–2.44 (m, 2H, $CH_2CH_2C(O)CH_3$), 2.23 (s, 3H, $C^3C(O)CH_3$), 2.25–2.09 (m, 3H, $C^4HH' + CH_2CH_2C(O)CH_3$), 2.14 (s, 3H, $CH_2CH_2C(O)CH_3$), 1.94–1.80 (m, 1H, C^5HH'), 1.80–1.66 (m, 1H, C^5HH''), 1.63–1.54 (m, 1H, C^4HH'). $^{13}C\{^1H\}$ NMR (100.6 MHz, $CDCl_3$): δ 208.02 ($C^3C(O)CH_3$), 207.05 ($CH_2CH_2C(O)CH_3$), 169.71 (C^2), 137.06 (*ipso*-arom), 128.78 (2C, *meta*-arom), 128.19 (2C, *ortho*-arom), 127.66 (*para*-arom), 59.25 (C^5), 50.81 (CH_2Ph), 47.52 (C^6H_2), 39.24 ($CH_2CH_2C(O)CH_3$), 30.08 ($CH_2CH_2C(O)CH_3$), 29.45 (C^4H_2), 29.42 ($CH_2CH_2C(O)CH_3$), 26.91 ($C^3C(O)C^7H_3$), 20.1 (C^5H_2). HPLC (Daicel CHIRALPACK OD-H, 0.7 mL/min, hexane/*i*-PrOH, 95:5): $t_R = 60.3$ min, 67.4 min, racemic. Analytical data are consistent with literature data.⁴²

2-(3,3-Dimethylbutyryl)-2-(3-oxobutyl)cyclopentanone (8i). R_f (silica gel 60, hexane/TBME, 4:1) = 0.2. 1H NMR (500 MHz, C_6D_6): δ 2.64 (d, $J_{H,H} = 17.37$ Hz, 1H, $C(O)CHH't-Bu$), 2.47–2.40 (m, 1H, CHH''), 2.32 (d, $J_{H,H} = 17.37$ Hz, 1H, $C(O)CHH''t-Bu$), 2.28–1.90 (m, 6H, $C^5H_2 + CH_2CH_2C(O)CH_3 + CH_2CH_2C(O)CH_3$), 1.73 (s, 3H, $CH_2CH_2C(O)CH_3$), 1.61–1.51 (m, 2H, C^3H_2), 1.11 (s, 9H, $C(O)CH_2C(CH_3)_3$). $^{13}C\{^1H\}$ NMR (125.8 MHz, C_6D_6): δ 215.43 (C^1), 205.68 ($C(O)CH_2t-Bu$), 205.49 ($CH_2CH_2C(O)CH_3$), 68.48 (C^2), 49.81 ($C(O)CH_2t-Bu$), 38.72 (C^5), 38.56 ($CH_2CH_2C(O)CH_3$), 31.83 ($CH_2CH_2C(O)CH_3$), 30.98 ($C(O)CH_2C(CH_3)_3$), 29.8 ($C(O)CH_2C(CH_3)_3$), 29.55 ($CH_2CH_2C(O)CH_3$), 28.04 (C^4), 19.7 (C^5). HPLC (Daicel CHIRALPACK AS, 0.5 mL/min, hexane/*i*-PrOH, 99:1): $t_R = 23.7$ min (major), 25.5 min (minor). Analytical data are consistent with literature data.^{6a}

Stoichiometric Reaction of 2a with Methyl Vinyl Ketone (7). Complex **2a** was prepared *in situ* by activation of **1** (30.0 mg, 36 μ mol) with $(Et_3O)PF_6$ (17.9 mg, 72 μ mol, 2.0 equiv) in CD_2Cl_2 (1 mL) in a Schlenk tube under argon during 18 h, after which **4a** (6.7 mg, 36 μ mol, 1.0 equiv) and decane (5.0 mg, 35 μ mol) were added. After 1 h of additional stirring, **7** (4 μ L, 49 μ mol, 1.3 equiv) was added. The reaction was monitored by GC analysis by taking samples (30 μ L) of the solution, which were quenched with Et_4NCl (~10 mg). After a total reaction time of 4 h, the conversion of **2** and the yield of **8a** were 98% and 93%, respectively. The enantiomeric excess of **8a** was 90% ee (by HPLC). The 1H NMR, GC-MS, and HPLC data were identical to those of the product of catalysis.

Stoichiometric Reaction of 3a with 7. Isolated enolato complex **3a** (57 mg, 52 μ mol) and methyl vinyl ketone (4.3 μ L, 52 μ mol, 1.0 equiv) were dissolved in CD_2Cl_2 (1 mL). The solution was

(39) Christoffers, J.; Rössler, U.; Werner, T. *Eur. J. Org. Chem.* **2000**, 701.

(40) Sasai, H.; Arai, T.; Shibasaki, M. *J. Am. Chem. Soc.* **1994**, *116*, 1571.

(41) Onimura, K.; Matsuzaki, K.; Lee, Y. -K.; Tsutsumi, H.; Oishi, T. *Polym. J.* **2004**, *36*, 190.

(42) Christoffers, J.; Kreidler, B.; Unger, S.; Frey, W. *Eur. J. Org. Chem.* **2003**, 2845.

transferred in a NMR tube and monitored by NMR spectroscopy. No reaction was detected after 48 h.

Reaction of 3a/Et₃NH⁺ with 7. [RuCl₂(PNNP)] (**1**) (100 mg, 0.12 mmol) and (Et₃O)PF₆ (62.7 mg, 0.25 mmol, 2.1 equiv) were dissolved in CD₂Cl₂ (1 mL), and the solution was stirred for 6 h, after which **4a** (26.6 mg, 0.14 mmol, 1.2 equiv) was added. After stirring the solution for an additional 6 h, NEt₃ (24 mg, 0.24 mmol, 2.0 equiv) and then **7** (12.2 mg, 0.17 mmol, 1.4 equiv) were added. The resulting solution was transferred in a NMR tube and monitored by NMR spectroscopy. No reaction was detected after 48 h.

Reaction of 3a with (HNEt₃)BPh₄ and 7. Enolato complex **3a** (19 mg, 18 μmol) was dissolved in CD₂Cl₂ (1 mL). (HNEt₃)BPh₄ (7 mg, 18 μmol, 1.0 equiv) and methyl vinyl ketone (1.5 μL, 18 μmol, 1.0 equiv) were added, and the solution was transferred in a NMR tube and monitored by NMR spectroscopy. No reaction was detected after 48 h.

Low-Temperature Protonation of 3a with Camphorsulfonic Acid. A solution of enolato complex **3a** (15 mg, 13.8 μmol) in dry CD₂Cl₂ (0.4 mL) was cooled to -90 °C in an NMR tube sealed with a Young valve. A solution of DL-10-camphorsulfonic acid (3.2 mg, 13.8 μmol, 1 equiv) in CD₂Cl₂ (0.1 mL) was added slowly. The tube was inserted into the NMR magnet precooled to -90 °C, then ¹H and ³¹P NMR spectra were recorded at various temperatures upon warming from -90 to 0 °C. The proton exchange rate constant k_{cT} at the coalescence temperature (-40 °C) was estimated from the frequency difference between the high-frequency doublets of **2a** (δ 61.43) and **3a** (δ 63.91) in the ³¹P NMR spectrum at 162.0 MHz according to the equation⁴³

$$k_{cT} = \frac{\pi}{\sqrt{2}} \cdot |\nu_{2a} - \nu_{3a}|$$

X-ray Structure of 3a. As all attempts to crystallize the enantiomerically pure (*S,S*)-**3a** failed, (*rac*)-**3a**¹⁶ was crystallized by slow diffusion of pentane into CH₂Cl₂. Crystal data for C₅₄H₅₅Cl₂F₆N₂O₃P₃Ru: prism (0.80 × 0.42 × 0.23 mm), triclinic, *P* $\bar{1}$, cell dimensions (200 K) $a = 14.9279(11)$ Å, $b = 16.6872(12)$ Å, $c = 23.5871(17)$ Å, $\alpha = 78.0510(10)^\circ$, $\beta = 74.0360(10)^\circ$, $\gamma = 79.2880^\circ$ and $V = 5474.5(7)$ Å³ with $Z = 2$, $D_c = 1.433$ Mg/m³, $\mu = 0.549$ mm⁻¹ (Mo K α , graphite monochromated), $\lambda = 0.71073$ Å, $F(000) = 2420$. The data were collected at 200 K on a Bruker AXS SMART APEX platform in the θ range 1.72–26.37°. The structure was solved with SHELXTL using direct methods. The asymmetric unit contains two essentially identical, crystallographically independent **3a** molecules, two crystallographically independent [PF₆]⁻ anions, and four disordered CH₂Cl₂ molecules at partial occupation (approximately total of 2.7). Of the 49 537 measured reflections with index ranges $-18 \leq h \leq 18$, $-20 \leq k \leq 20$, $-29 \leq l \leq 29$, 22 319 independent reflections were used in the refinement (full-matrix least-squares on F^2 with anisotropic displacement parameters for all non-H atoms, except C(4S) of a disordered CH₂Cl₂ molecule). Hydrogen atoms were introduced at calculated positions and refined with the riding model and individual isotropic thermal parameters for each group. Final residuals were $R_1 = 0.0497$ (for 19 304 reflections with $I > 2\sigma(I)$), $R_1 = 0.0573$ (all data), $wR_2 = 0.1418$ (all data), GOF = 1.041. Max. and min. difference peaks were +2.25 and -0.73 e Å⁻³, the largest and mean $\Delta/\sigma = 0.001$ and 0.000.

X-ray Structure of 3h. As all attempts to crystallize the enantiomerically pure complex (*S,S*)-**3h** failed, (*rac*)-**3h**¹⁶ was crystallized by slow diffusion of hexane into CH₂Cl₂. Crystal data for C₆₁H₅₂Cl₆F₆N₃O₂P₃Ru: prism (0.24 × 0.21 × 0.14 mm), triclinic, *P* $\bar{1}$, cell dimensions (220 K) $a = 11.8816(12)$ Å, $b = 16.0042(17)$ Å, $c = 16.4275(17)$ Å, $\alpha = 96.802(2)^\circ$, $\beta = 97.407(2)^\circ$, $\gamma = 93.830(2)^\circ$ and $V = 3065.2(5)$ Å³ with $Z = 2$, $D_c = 1.495$ Mg/m³, $\mu = 0.659$ mm⁻¹ (Mo K α , graphite monochromated), $\lambda = 0.71073$ Å, $F(000) = 1400$. The data were collected at 220 K on a Bruker AXS SMART APEX platform in the θ range 1.29–26.37°. The structure was solved with SHELXTL using direct methods. The asymmetric unit contains one **3h** cation, one [PF₆]⁻ anion, and three disordered CH₂Cl₂ molecules. The six-membered ring of the lactam has an envelope conformation with the out-of-plane atom, C(49), disordered over two positions at 87:13 occupancy (only the major conformer is shown in the ORTEP plot). Of the 25 128 measured reflections with index ranges $-14 \leq h \leq 14$, $-20 \leq k \leq 19$, $-20 \leq l \leq 20$, 12 434 independent reflections were used in the refinement (full-matrix least-squares on F^2 with anisotropic displacement parameters for all non-H atoms). Hydrogen atoms (of non-H atoms) were introduced at calculated positions and refined with the riding model and individual isotropic thermal parameters for each group. Final residuals were $R_1 = 0.0620$ (for 9525 reflections with $I > 2\sigma(I)$), $R_1 = 0.0848$ (all data), $wR_2 = 0.1924$ (all data), GOF = 1.058. Max. and min. difference peaks were +1.59 and -1.03 e Å⁻³, the largest and mean $\Delta/\sigma = 0.001$ and 0.000.

X-ray Structure of 6. Orange crystals of (*rac*)-**6**¹⁶ were obtained by slow diffusion of toluene into a CD₂Cl₂ solution of (*rac*)-**2a**. Crystal data for C₅₀H₄₈BF₆N₂O₅P₃Ru: prism (0.475 × 0.475 × 0.321 mm), monoclinic, *P*₂₁/*n*, cell dimensions (200 K) $a = 12.0460(5)$ Å, $b = 20.6031(9)$ Å, $c = 20.3481(9)$ Å, $\beta = 92.7020(10)^\circ$, and $V = 5044.5(4)$ Å³ with $Z = 4$, $D_c = 1.416$ Mg/m³, $\mu = 0.475$ mm⁻¹ (Mo K α , graphite monochromated), $\lambda = 0.71073$ Å, $F(000) = 2200$. The data were collected at 200 K on a Bruker AXS SMART APEX platform in the θ range 1.41–26.03°. The structure was solved with SHELXTL using direct methods. Of the 44 016 measured reflections with index ranges $-14 \leq h \leq 14$, $-25 \leq k \leq 25$, $-25 \leq l \leq 25$, 9948 independent reflections were used in the refinement (full-matrix least-squares on F^2 with anisotropic displacement parameters for all non-H atoms). Hydrogen atoms (of non-H atoms) were introduced at calculated positions and refined with the riding model and individual isotropic thermal parameters for each group. The acidic hydrogen H(3A) was located in the electron density map and refined with restrained O–H distances. O(3)–H(3A), 1.135(16); O(6)⋯H(3A), 1.515(18); O(3)⋯O(6), 2.641(17) Å; O(3)–H(3A)⋯O(6), 170(8)°; H(3A)–O(6'), 1.551(19), O(3)⋯O(6), 2.651(17) Å; O(3)–H(3A)⋯O(6'), 161(6)°. Final residuals were $R_1 = 0.0545$ (for 8604 reflections with $I > 2\sigma(I)$), $R_1 = 0.0631$ (all data), $wR_2 = 0.1606$ (all data), GOF = 1.116. Max. and min. difference peaks were +0.92 and -0.466 e Å⁻³, the largest and mean $\Delta/\sigma = -0.0041$ and 0.000.

Acknowledgment. We thank Dr. Heinz Rügger for his assistance with NMR spectroscopy.

Supporting Information Available: CIF files of **3a**, **3h**, and **6**. This material is available free of charge via the Internet at <http://pubs.acs.org>.

OM800197Y

(43) Sandström, J. *Dynamic NMR Spectroscopy*; Academic Press: London, 1982; p 79.